Preprint PUP-TH-1544 (1995) and LANCS-TH/9517 (1995) e-Print Archive: hep-ph/9506475

How fast can the wall move?

A study of the electroweak phase transition dynamics

Guy D. Moore¹

Princeton University
Joseph Henry Laboratories, PO Box 708
Princeton, NJ 08544, USA

and

Tomislav Prokopec²

Lancaster University
School of Physics and Chemistry
Lancaster LA1 4YB, UK

Abstract

We consider the dynamics of bubble growth in the Minimal Standard Model at the electroweak phase transition and determine the shape and the velocity of the phase boundary, or bubble wall. We show that in the semi-classical approximation the friction on the wall arises from the deviation of massive particle populations from thermal equilibrium. We treat these with Boltzmann equations in a fluid approximation. This approximation is reasonable for the top quarks and the light species while it underestimates the friction from the infrared W bosons and Higgs particles. We use the two-loop finite temperature effective potential and find a subsonic bubble wall for the whole range of Higgs masses $0 < m_H < 90 \text{GeV}$. The result is weakly dependent on m_H : the wall velocity v_w falls in the range $0.36 < v_w < 0.44$, while the wall thickness is in the range 29 > LT > 23. The wall is thicker than the phase equilibrium value because out of equilibrium particles exert more friction on the back than on the base of a moving wall. We also consider the effect of an infrared gauge condensate which may exist in the symmetric phase; modelling it simplemindedly, we find that the wall may become supersonic, but not ultrarelativistic.

1 Introduction

It has gradually become clear that the baryon asymmetry of the universe may have been created at a first order electroweak phase transition. The most important ingredient, baryon number violation, was demonstrated in the Standard Model by t'Hooft [1] and was later shown to proceed rapidly at high temperatures [2, 3]. The necessary departure from thermal equilibrium is supplied by the first order electroweak

¹e-mail: guymoore@puhep1.princeton.edu

²e-mail: T.Prokopec@lancaster.ac.uk, address from Sep 1 '95: Cornell University

phase transition [4], which has recently been the subject of intense investigation [5, 6, 7, 8, 9, 10, 11]. There have also been promising developments in understanding the mechanisms by which baryogenesis may proceed.

The general picture is this: at high temperatures, such as those prevalent in the early universe, thermal effects prevent the breaking of electroweak symmetry by the Higgs mechanism. As the universe expands and the temperature falls, the plasma supercools in this "symmetric" phase until the probability of bubble nucleation is large enough that bubbles of the lower temperature "asymmetric" phase, in which a Higgs field condensate breaks electroweak symmetry, form. These bubbles are thermodynamically favorable, so they expand, converting the symmetric phase into the asymmetric phase. At the bubble surfaces, where the phase conversion occurs, the plasma is thrown out of equilibrium by the motion of the phase boundary, or bubble wall. Inside the bubbles, baryon number is approximately conserved; outside it is rapidly violated. If the departure from equilibrium on the bubble surface biases the rate of baryon number violation in a CP violating fashion, this produces a baryon asymmetry.

Specific mechanisms address how the motion of the bubble wall biases the baryon number violating processes. The most efficient mechanisms rely on transport. The bubble wall separates particles and their antiparticles in a CP violating fashion. In the thin wall case this occurs through CP violating quantum mechanical reflection [12, 13, 14], while in the thick wall case the energy levels of particles and their antiparticles split in the presence of a CP violating condensate, leading to a different perturbation in the population densities of particles and antiparticles [15, 16, 17]. The difference between particle and antiparticle populations is then transported into the symmetric phase, where it biases the baryon number violation rate. The models based on transport, like most, depend intimately on the details of the bubble wall shape and its motion. If the bubble wall is very thin, quantum mechanical reflection is the correct language; if it is very thick, scatterings are frequent, and the problem should be viewed semi-classically. Correctly describing the situation where the wall is thin in comparison to the de Broglie wavelength of some particles, but thick enough that particles scatter frequently on the wall, is still an open problem. In the thin wall case the main effect comes from the low-momentum particles while in the thick wall case the effect from thermal particles dominates. The efficiency of transport strongly depends on the velocity and thickness of the wall. For instance, for a slow wall, particles diffuse far in front of the wall, and nonlocal baryogenesis is possible. For a thin and supersonic wall a typical reflected particle travels about one diffusion length ahead of the wall, while for a thick and fast wall no forward transport is possible. In the latter case only local baryogenesis occurs, i.e. CP violation and baryon violation take place at the same point in space. In any case it is clearly of crucial importance to know the shape and velocity of the expanding bubble wall.

While there has been substantial progress on this problem [18, 5, 19, 20, 21], much remains to be done to compute the wall velocity and shape reliably. In particular, no work fully addresses the following issues: (a) infrared boson populations; (b) effects of transport; (c) systematic treatment of all relevant scattering and decay diagrams to leading order; (d) change in velocity and temperature of the plasma due to latent heat

release; (e) dynamical determination of the wall shape (thickness). In a recent letter [22] we developed a set of techniques and approximations which address (b), (c), and (e). In this paper we present the details of that work and extend it to include (d). The problem of infrared boson populations is of theoretical interest, since it is related to the infrared properties of gauge theories at finite temperature, which are not well understood. We leave the proper treatment of this problem to a future work. The fluid approximation we use probably underestimates the friction from infrared bosons, so our result could be interpreted as an upper bound for the wall velocity. Also note that we work within the Minimal Standard Model, even though extensions with more CP violation are generally considered more viable candidates for baryogenesis. We do this for simplicity, developing the techniques to control the problem before we attempt to apply them to more complicated and interesting models.

Now let us briefly outline the paper. In section II, we derive a semi-classical equation of motion for the Higgs condensate in the presence of out of equilibrium particle populations. The semi-classical approximation is accurate provided the scale on which the Higgs field condenses, given by the wall thickness, is large in comparison to the inverse momentum scale of particles which significantly contribute to friction. Solving this equation requires knowledge of the effective potential, the temperature at the wall, and the departure of particle populations from equilibrium in the presence of the wall. In section III we review the state of the art in the effective potential. In section IV, we study the bubble nucleation using Langer's formalism and the potential of section III. This formalism was applied to the field theory by Coleman and Callan in [23] and to the electroweak phase transition in [24, 18, 5, 19, 25] and permits the calculation of the temperature at which the bubbles nucleate.

The liberation of latent heat produces a jump in temperature and velocity across the wall, and changes the temperature behind the wall with respect to the temperature far from the bubble. We compute this effect using stress-energy conservation, as done for example in [24, 19, 26]. Including this effect could be important since it may significantly increase the friction on the wall, especially when the wall velocity approaches the speed of sound. This is an important improvement on our work in [22], where for simplicity we ignored this effect.

Next, we address the departure of particle populations from equilibrium in the presence of the wall. In section V we solve exactly a particularly simple case of free particle scatterings off the wall (assuming efficient diffusion so that no piling up occurs in front of the wall). Unfortunately this is a reasonable approximation only for an unrealistically thin wall. However, it does help us to determine what aspects of the departure from equilibrium are most important. For fermions we find that most of the friction arises from thermal energy particles, while for bosons most arises from infrared particles. The friction depends on a particle's mass as m^4 , so top quarks appear to be the largest contributors to the friction, even though they are scattered fairly efficiently. This justifies the development of an approximation for the particle populations which models thermal particles reasonably accurately. This is the fluid approximation, which is developed in some detail in section VI, with a systematic study of the leading order tree-level processes that restore equilibrium postponed to Appendix A. Section VII studies aspects of transport in the fluid equations by

finding the response to a δ -function source. It is shown that, in contrast to a slow wall, no forward transport is possible for a supersonic wall. The accuracy of and possible improvements to the fluid approximation within the context of a momentum expansion are discussed in Appendix B.

Finally, we combine the fluid approximation with the equation of motion for the Higgs field and solve for the bubble velocity and profile. In spite of the nonlinear character in the equation of motion, this system of equations can be solved analytically using the Fourier transform and a two parameter Ansatz for the wall shape, as we show in section VIII. In section IX we describe a numerical technique which allows a general wall profile. The results are presented in section X. The numerical work shows that the Ansatz models the wall velocity with good accuracy (typically within 5%) although it is not as good at modelling the wall profile, as illustrated in Figure 3. We conclude that the Ansatz technique is reasonably accurate for subsonic wall velocities. However, for very supersonic velocities, which may occur if infrared physics generates gauge condensates in the symmetric phase, both the Ansatz, and the fluid approximation itself, break down. This is discussed in Appendix C, where it is shown that the bubble wall cannot propagate as an ultrarelativistic detonation.

For the impatient reader we suggest a fast track to reading the paper: section II, the second half of section IV, section VI, and sections VIII - X.

2 Equation of motion

We are interested in the dynamics of an infrared Higgs condensate, which we will treat as a classical background field. From the terms in the Electroweak Lagrangian containing Φ ,

$$\mathcal{L} = (\mathcal{D}_{\mu}\Phi)^{\dagger}\mathcal{D}^{\mu}\Phi + \mu\Phi^{\dagger}\Phi - \lambda(\Phi^{\dagger}\Phi)^{2} - \sum y(\Phi^{\dagger}\overline{\psi_{R}}\psi_{L} + \Phi\overline{\psi_{L}}\psi_{R})$$

where the sum is over all massive fermions and y is the Yukawa coupling, we derive the operator equation of motion

$$\Box \hat{\Phi} + ig\hat{A}^{\mu}\partial_{\mu}\hat{\Phi} + \frac{ig}{2}(\partial \cdot \hat{A})\hat{\Phi} - \frac{g^{2}}{4}\hat{A}^{2}\hat{\Phi} - \mu\hat{\Phi} + 2\lambda(\hat{\Phi}^{\dagger}\hat{\Phi})\hat{\Phi} + \sum y\hat{\psi}_{R}\hat{\psi}_{L}$$

We have suppressed group indices. Each term containing A actually appears once for weak isospin and once for hypercharge.

This operator should annihilate the physical thermal state. We will shift Φ by a classical part, $\Phi = \Phi_{cl} + \delta\Phi$, choosing $\delta\Phi$ such that $\langle \delta\Phi \rangle = 0$. We then evaluate the trace of the operator equation of motion over the (out of equilibrium) thermal density matrix describing the propagating bubble wall. We will assume that there are no charge conjugation violating gauge condensates, so that $\langle A^{\mu} \rangle = 0$. We then find

$$\Box \Phi_{cl} - \mu \Phi_{cl} + 2\lambda (\Phi_{cl}^{\dagger} \Phi_{cl}) \Phi_{cl} +$$

$$2\lambda \left(2\langle \delta \Phi^{\dagger} \delta \Phi \rangle \Phi_{cl} + \langle \delta \Phi^{2} \rangle \Phi_{cl}^{\dagger} \right) - \frac{g^{2}}{4} \langle A^{2} \rangle + \sum y \langle \overline{\psi}_{R} \psi_{L} \rangle = 0$$

We assume that $\Phi_{cl} = [0 \ \phi/\sqrt{2} \]^T$ (which is the same as neglecting charge conjugation violating condensates). Next, we evaluate the thermally averaged operators using WKB wave functions. This makes sense because the background field ϕ varies on a scale much longer than T^{-1} , which characterizes the reciprocal momenta of particles in the plasma. In this approximation,

$$\langle A^2 \rangle = \langle A_{vac}^2 \rangle + \sum \int \frac{d^3k}{(2\pi)^3 E} f(k, x)$$

where the sum is over group indices and spins and f is the phase space population density, and

$$\langle \overline{\psi_R} \psi_L \rangle = \frac{1}{2} \langle \overline{\psi} \psi \rangle_{vac} + \sum \int \frac{d^3k}{(2\pi)^3} \frac{m}{2E} f(k, x)$$

where the sum is over group and Dirac indices.

The equation of motion becomes

$$\Box \phi + V'(\phi) + \sum \frac{dm^2}{d\phi} \int \frac{d^3k}{(2\pi)^3} \frac{1}{2E} f(k, x) = 0$$
 (1)

where V is the renormalized vacuum potential, and the sum includes all massive physical degrees of freedom, including the high frequency parts of the Higgs field. Note the condensed notation: $m^2 = y^2\phi^2/2$ for quarks and leptons, $g_w^2\phi^2/4$ for the gauge fields, $3\lambda\phi^2 - \mu$ +(thermal) for the Higgs bosons, and $\lambda\phi^2 - \mu$ +(thermal) for the pseudo-Goldstone modes. This equation has also been derived by diagrammatic techniques in [19].

This equation has a nice physical interpretation. Multiplying it by $\partial^{\mu}\phi$, we find

$$0 = \Box \phi \partial^{\mu} \phi + \partial^{\mu} V + \int \frac{d^3 k}{(2\pi)^3 2E} f(k) \partial^{\mu} m^2$$
 (2)

The first term can be recast as $\partial_{\mu}\partial^{\mu}\phi\partial^{\nu}\phi = \partial_{\mu}(\partial^{\mu}\phi\partial^{\nu}\phi) - \partial^{\nu}(\partial_{\mu}\phi\partial^{\mu}\phi/2)$, so that when taken together the first two terms are the divergence of the stress-energy of the Higgs field $T^{\mu\nu}(\phi) = \partial^{\mu}\phi\partial^{\nu}\phi - g^{\mu\nu}\mathcal{L}(\phi)$, where $\mathcal{L}(\phi) = \partial^{\mu}\phi\partial_{\mu}\phi/2 - V(\phi)$ is the Higgs lagrangian. The last term represents exchange of stress-energy with particles; it looks like $\int d^3k f(k)(-F^{\mu})/(2\pi)^3$. Here $F^{\mu} = -\partial^{\mu}E = (-\partial_t E, -\nabla E)$ is the 4-force a particle feels in the presence of the wall; the wall feels an equal and opposite force. Thus we can recast (2) as follows

$$\partial_{\nu}T^{\nu\mu}(\phi) - \int \frac{d^3k}{(2\pi)^3} f(k)F^{\mu} = 0, \qquad F^{\mu} = -\partial^{\mu}E$$
 (3)

The equation of motion for the Higgs field in the WKB approximation splits the total (conserved) stress-energy tensor $T^{\mu\nu}$ into Higgs and fluid parts (*sub-systems*) in a natural way, and provides the prescription for how each is violated.

As an application of (3), $\int (\text{Eq.1})\phi'dz$ is the total pressure on the wall. If this integral does not vanish, then the wall accumulates momentum and accelerates; hence

this integral must vanish for a steady state wall. This fact forms the basis of the analysis of [18, 5, 19].

We write the population density f as the equilibrium population f_0 plus a deviation, $f = f_0 + \delta f$. The vacuum contribution $V'(\phi)$ and the contribution from f_0 combine to give the finite temperature effective potential $V'_T(\phi)$. Thus we have

$$\Box \phi + V_T'(\phi) + \sum \frac{dm^2}{d\phi} \int \frac{d^3p}{(2\pi)^3 2E} \delta f(p, x) = 0$$
 (4)

If the system were in phase equilibrium we would have expected $\Box \phi + V_T'$; we see that the frictive force (dissipation) arises due to the departure from thermal equilibrium δf (fluctuation). Our goal will be to solve this equation for a stationary wall, *i.e.* after the wall has reached a steady shape and velocity. To do so we need to know the effective potential V_T and the temperature T, and we need a way to calculate δf .

3 Effective Potential

The high temperature expansion of the one loop effective potential, ignoring scalar loops, is [5]

$$V(\phi, T) = D(T^2 - T_o^2)\phi^2 - ET\phi^3 + \frac{\lambda_T}{4}\phi^4.$$
 (5)

Here

$$D = \frac{1}{8v_o^2} (2m_W^2 + m_Z^2 + 2m_t^2) \sim 0.169 ,$$

$$E = \frac{1}{4\pi v_o^3} (2m_W^3 + m_Z^3) \sim 10^{-2} ,$$

$$T_o^2 = \frac{1}{4D} (m_H^2 - 8Bv_o^2) ,$$

$$\lambda_T = \frac{m_H^2}{2v_o^2} - \frac{3}{16\pi^2 v_o^4} \left(2m_W^4 \ln \frac{m_W^2}{a_B T^2} + m_Z^4 \ln \frac{m_Z^2}{a_B T^2} - 4m_t^4 \ln \frac{m_t^2}{a_F T^2} \right) ,$$
 (6)

where $\ln a_B = 2 \ln 4\pi - 2\gamma \simeq 3.91$, $\ln a_F = 2 \ln \pi - 2\gamma \simeq 1.14$, and

$$B = \frac{3}{64\pi^2 v_o^4} (2m_W^4 + m_Z^4 - 4m_t^4)$$

The value of ϕ in the broken phase at equilibrium is easily evaluated to be $2ET/\lambda_T$. If we take λ_T parametrically $\sim g^2$, which is natural from the renormalization structure of the standard model, we find $\phi \sim gT$, which is small enough that the perturbation series may not be well behaved [27]. We should therefore include the two loop contribution, which has recently been computed by [6] and [7]. The two loop expression contains terms $\sim g^4\phi^2T^2$, with a coefficient including constants and logs of the temperature over the renormalization scale, which slightly corrects D. We will drop this term as it has no influence on the behavior of the phase transition. Two more important corrections do occur, however. One is that the longitudinal components

of the gauge bosons acquire large plasma masses [28, 5] and do not contribute to the strength of the transition. Following [5] we drop them from the E term in the effective potential, giving

$$E = \frac{1}{12\pi} (4m_W^3 + 2m_z^3 + (3+3^{1.5})\lambda_T^{1.5})$$

where the λ_T dependent term comes from including ring improved scalar loops. The other correction is that qualitatively new terms $\sim g^4\phi^2T^2\ln(m/T)$ appear. Here m stands for sums of masses of particles. In the approximation that the Higgs masses are small in the symmetric phase (which should be good near the transition temperature) we may treat $m \sim g\phi$; the log of g is absorbed into D, and the new term becomes $-C\phi^2T^2\ln(\phi/T)$. The value of the coefficient is [7]

$$C \simeq \frac{1}{16\pi^2} (1.42g_w^4 + 4.8g_w^2 \lambda_T - 6\lambda_T^2)$$

where we have again left out contributions from transverse gauge bosons. Including this term, the value of ϕ in the broken phase at equilibrium becomes $\phi/T = E/\lambda_T + \sqrt{(E/\lambda_T)^2 + 2C/\lambda_T}$, which indicates that the new term strengthens the transition and contributes at the same parametric order as the one loop term E, although for the parameters we will be interested in its contribution is smaller.

Because the two loop result is of the same parametric order as the one loop result we might worry that perturbation theory cannot establish the strength of the transition reliably. In fact we expect that the perturbative computation of the effective potential should break down in the symmetric phase. This means that the value of $V_T(0)$ may be shifted somewhat from zero. Shaposhnikov has suggested that such a shift may arise due to the formation of gauge condensates in the symmetric phase [8]. He advocates adding a term $-A_F g^6/12 * \text{Pit}(\phi)$ to the effective potential to account for such an effect. Here the function Pit describes the ϕ dependence of the strength of such a condensate, and is smooth at $\phi = 0$ but falls as $\exp(-\phi/g^2)$ at larger ϕ . We will include such a contribution to parametrize our ignorance of the effective potential in the symmetric phase. We choose Pit= $\operatorname{sech}(\phi/\alpha_W)$ because it is simple, but our results do not depend strongly on the functional form or the exact rate of exponential decay, as long as that decay is rapid. We treat the value of A_F as an unknown parameter; there is some lattice evidence for its value but it is still preliminary [9, 11].

Our final form for the effective potential is then

$$V_T(\phi) = D(T^2 - T_0^2)\phi^2 - CT^2\phi^2 \ln(\frac{\phi}{T}) - ET\phi^3 + \frac{\lambda_T}{4}\phi^4 - \frac{A_F g^6}{12} \operatorname{sech}(\frac{\phi}{\alpha_W})$$
 (7)

4 Nucleation and Hydrodynamics

We must next determine what T is at the bubble wall. Following [18, 24] we do this in two steps; first we calculate the temperature in the universe when most bubble

nucleation events occur, and then we calculate the temperature correction due to the release of latent heat by the bubble as it expands.

The process of bubble nucleation at finite temperature was worked out by Linde [29] and applied to the electroweak phase transition in [24, 18, 5, 30, 19, 25]. The basic idea is that small bubbles are thermodynamically unfavorable because of positive surface free energies; to become large enough not to re-contract a bubble must pass over a free energy barrier. The lowest route over the barrier goes through a saddlepoint configuration of the effective action called the critical bubble. It is a spherically symmetric solution to the classical equilibrium equation of motion

$$\nabla^2 \phi(r) = V_T'(\phi)$$
 $\phi'(r=0) = 0$, $\phi(\infty) = 0$ (8)

The free energy of such a solution is

$$S_{\text{crit}} = \int d^3x \left(\frac{1}{2} (\nabla \phi)^2 + V_T(\phi) \right) \tag{9}$$

There are analytic formulas for S_{crit} only in special cases; in general it must be determined numerically.

The nucleation rate per unit volume per unit time is

$$\frac{\Gamma}{V} = I_0 T^4 \exp(-\frac{S_{\text{crit}}}{T}) \tag{10}$$

Carrington and Kapusta have recently computed the prefactor [25]. Numerically evaluating the expressions in their paper we find, roughly, $\ln(I_0) \simeq -14$. The exact value depends on the parameters of the effective potential and (weakly) on temperature, but as we will see we only need a rough estimate.

We can now compute the action of the critical bubble at the time when most of the universe changes phase by following the technique of [30]. If bubbles expand at a velocity v_w which depends only weakly on temperature, then the fraction of space remaining in the symmetric phase at time t is roughly

$$\exp\left(-\int_{-\infty}^{t} \frac{4\pi}{3} v_w^3 (t - t')^3 I_0 e^{-S(t')/T} dt'\right) \tag{11}$$

where the exponential accounts for bubble overlap [31]. Expanding the bubble action about the point when the above integral is 1, $S = S(T_{\text{nuc}}) + (t - t')dS/dt$ and using d/dt = (dT/dt)d/dT and (1/T)dT/dt = H the Hubble constant, we find that most of space has changed phase when

$$e^{S(T_{\text{nuc}})/T} = \frac{8\pi v_w^3 I_0}{(HTdS/dT)^4}$$

A reasonable estimate for TdS/dT is the thin wall value $2ST/(T_{\rm eq}-T) \sim 10^4$, which roughly agrees with the value we find by numerically evaluating S/T at closely spaced values of T. The value of H follows from the Friedmann equation

$$H^2 = \frac{8\pi G}{3} \, \frac{\pi^2 g_* T^4}{30}$$

where the second factor is the energy density of the plasma and $g_* = 106.75(1+O(\alpha_s))$ in the symmetric phase (the $O(\alpha_s)$ arises from thermal masses and other interaction effects). The value of v_w is to be determined, but since a subsonic bubble is proceeded by a hydrodynamic front travelling at the speed of sound which raises the temperature of the fluid and prevents nucleation, it is sensible to choose the speed of sound $v_s = 1/\sqrt{3}$.

Putting all the expressions together and using $T \sim 100 \text{GeV}$, we find $S/T \simeq 97$. In Ref. [30] a slightly higher value was found because of the value for I_0 we use. We may now determine the temperature at which most nucleation occurs by solving (8) for various values of T until we find one which gives $S_{\text{crit}} = 97$.

This gives the temperature around the bubble at the time that it nucleates, but we are really interested in the temperature at the bubble wall while it is expanding. This will be elevated from T_{nuc} because of the liberation of latent heat as the symmetric phase is converted into the asymmetric phase.

In [18, 5, 19] it is argued that the elevation of temperature at the bubble wall is not important in determining its velocity. This is true when the change in temperature, which is $\sim l/(d\rho/dT)$ (where l is the latent heat), is small compared to the supercooling, $T_{\rm eq} - T_{\rm nuc}$. [18, 19] show explicitly that for the effective potential they consider, $(T_{\rm eq} - T_{\rm nuc})(d\rho/dT)$ is about 5 times l. However, that analysis is based on a small assumed value of m_t ; the latent heat depends on $D \propto m_t^2$, and the supercooling $T_{\rm eq} - T_o \propto 1/D$; so for $m_t \simeq 174 {\rm GeV}$, the temperature increase probably is important.

To compute the temperature at the wall we need to solve the temperature profile around an expanding bubble wall. The equation of state in the symmetric phase is $\rho_s = (\pi^2 g_*/30)T^4$, $p_s = \rho_s/3$, and in the broken phase it is $\rho_a = \rho_s + l(T)$, $p_a = p_s - V_T(\phi(T))$. Here l is the latent heat and is given by

$$l = V_T(\phi_a) - T \frac{dV_T(\phi_a)}{dT} = -D\phi^2(T^2 + T_o^2) + (\frac{\lambda_T}{4} - B)\phi^4 \simeq -2D\phi^2T^2$$
 (12)

Note that $l/\rho \sim 0.01 << 1$, and similarly we find $(T_{\rm eq} - T)/T \sim 0.01 << 1$, so it is reasonable to expand to lowest order in these quantities. However, l turns out to be quite a strong function of temperature,

$$T\frac{d(l/T^4)}{dT} \simeq -4D\frac{\phi}{T}\frac{T\,d(\phi/T)}{dT} \tag{13}$$

We can determine $Td(\phi/T)/dT$ in the broken phase as follows; the value of ϕ is determined by $V'_T(\phi) = 0$, and since nonperturbative effects are tiny in the broken phase we can use the two loop expression, which gives

$$0 = 2D(T^{2} - T_{o}^{2})\phi - C\phi^{2}T^{2}(2\ln\frac{\phi}{T} + 1) - 3E\phi^{2}T + \lambda_{T}\phi^{3}$$

$$0 = 2D(1 - \frac{T_{o}^{2}}{T^{2}}) - 2C\ln\frac{\phi}{T} - C - 3E\frac{\phi}{T} + \lambda_{T}\left(\frac{\phi}{T}\right)^{2}$$
(14)

Since this equals zero, its total derivative with respect to T, $\partial/\partial T + d(\phi/T)/dT$ $\partial/\partial(\phi/T)$, should vanish. This gives

$$\frac{d(\phi/T)}{dT} = \frac{-4DT_o^2\phi/T}{2\lambda_T\phi^2 - 3E\phi T - 2CT^2} \tag{15}$$

and hence

$$T\frac{d(l/T^4)}{dT} \simeq -\frac{4D\phi}{T} \frac{-4DT_o^2\phi/T}{2\lambda_T\phi^2 - 3E\phi T - 2CT^2}$$
 (16)

For typical values of $\lambda_T = 0.03$, $\phi = 0.8$, we find $Td(l/T^4)/dT \simeq 18$, which is about half as large as ρ/T^4 . This rather surprising result occurs because ϕ is strongly temperature dependent in the broken phase near the transition, and because the top quark is so massive; around the transition temperature the number of top quarks is rapidly freezing out. Because ρ turns out to have this extra temperature dependence, the speed of sound in the broken phase, $dp/d\rho = (dp/dT)/(d\rho/dT)$, is around 15% smaller than in the symmetric phase. Thus it is reasonable to expand to linear order in l/ρ and $(T - T_{eq})/T$, and hence in δT and v, but not to neglect dl/dT.

Now let us explore the fluid temperature and velocity in the vicinity of an isolated spherical bubble. From Eq. (11) and the argument which follows, we find that the typical bubble grows to a radius of $\sim 1/(HTdS/dT) \sim 10^{12}/T$, while the distance it takes for a bubble to accelerate to a steady velocity is around the ratio of the surface tension to the free energy density difference of the two phases, which is of order 50/T. On the scale of the bubble radius, then, we can treat the plasma as a perfect fluid and expect the temperature and velocity to be functions of $r/t \equiv x$ only, where time t is measured from the time of nucleation. Conservation of the stress energy tensor gives the equations

$$0 = \partial_{\mu} T^{\mu\nu} = \partial_{\mu} ((\rho + p)u^{\mu}u^{\nu} - pg^{\mu\nu}) = u^{\nu}u \cdot \partial(\rho + p) + (\rho + p)(u^{\nu}\partial \cdot u + u \cdot \partial u^{\nu}) - \partial^{\nu} p \quad (17)$$

which to linear order in v and δT (which are linear in l/ρ) give

$$(\rho + p)\left(\frac{2}{x}v + \frac{dv}{dx}\right) - x\frac{d\rho}{dT}\frac{dT}{dx} = 0 \qquad \frac{dp}{dT}\frac{dT}{dx} = (\rho + p)x\frac{dv}{dx}$$
(18)

The 2v/x arises from taking a divergence in spherical coordinates and is the only difference between the spherical geometry and the planar geometry studied by [24, 19].

Because the equation of state for the symmetric phase is simple we can solve the above equations for the case that the wall velocity is less than the speed of sound in the broken phase (in which case T is constant and v is zero inside the bubble). The equations become

$$x\frac{dv}{dx} = \frac{d\ln T}{dx} \qquad 2v + x\left(1 - \frac{x^2}{v_s^2}\right)\frac{dv}{dx} = 0 \tag{19}$$

which give

$$v = A\left(1 + \frac{v_s}{x}\right)\left(1 - \frac{v_s}{x}\right) \qquad \ln\frac{T}{T_{\text{nuc}}} \simeq \frac{T - T_{\text{nuc}}}{T_{\text{nuc}}} = 2Av_s\left(1 - \frac{v_s}{x}\right)$$
 (20)

Here A is an undetermined parameter and $v_s = 1/\sqrt{3}$. It is interesting to note that, in this approximation (linear order in l/ρ), the temperature and velocity are actually continuous at $x = v_s$, although the first derivative is discontinuous. This holds to all perturbative orders in l/ρ . The shock front is exponentially weak, as found in [26].

Since the wall does not accumulate energy or momentum, Eq. (18) also provides us with boundary conditions at the bubble wall, by replacing the derivatives with differences. Because the wall is thin compared to the bubble radius the term 2v/x is negligible and we get

$$(\rho_s + p_s)v - v_w \rho_s = -v_w \rho_a(T_{\text{inside}}) \qquad -v_w(p_s + \rho_s)v + p_s = p_a(T_{\text{inside}})$$
 (21)

which, at fixed v_w , allows us to solve for the temperature in front of and behind the wall. Defining $y = v_w/v_s$, we find

$$\frac{T_s - T_{\text{nuc}}}{T_{\text{nuc}}} = \frac{y^2 l(T_a)}{2(1+y)^2 (1-y)} \qquad \frac{T_a - T_{\text{nuc}}}{T_{\text{nuc}}} = \frac{y^2 l(T_a)}{4(1+y)^2}$$
(22)

Note the dependence of l on T_a the temperature inside the bubble, which makes these equations transcendental.

When the wall velocity exceeds v_s , the only causal solution to (19) outside the bubble is v = 0, $T = T_{\text{nuc}}$. We may find the temperature just inside the bubble wall directly from the boundary conditions

$$(\rho_a + p_a)v - v_w \rho_a = -v_w \rho_s (T_{\text{nuc}}) \qquad -v_w (\rho_a + p_a)v + p_a = p_s (T_{\text{nuc}})$$
 (23)

which give

$$\frac{T_a - T_{\text{nuc}}}{T_{\text{nuc}}} = \frac{y^2 l(T_a)}{4(y+1)(y-1)}$$
 (24)

In both cases the temperature is elevated on one or both sides of the bubble. The elevation has a 1/(y-1) behavior, which diverges near v_s . This divergence means that our expansion in small v and $T-T_{\text{nuc}}$ must break down very near v_s ; but there is still a very large elevation in temperature when $v \simeq v_s$. As the symmetric phase becomes more favorable at higher temperatures this prevents the wall from propagating close to the speed of sound; it must either be a deflagration or a strong detonation.

We have not treated the case where v_w lies between v_s and the speed of sound in the broken phase; this case is much more complicated because the fluid velocity is nonzero on both sides of the wall and we need three conditions to determine all unknowns. Fortunately, in this case the temperature would be elevated enough that the wall probably cannot propagate at this speed; so we will not treat this case. We will also not treat the effect of latent heat released by other bubbles, although as the phase transition progresses and bubbles begin to collide, one bubble's wall will frequently be in the hydrodynamic wave initiated by another bubble. These effects make the later phases of the transition quite complicated, and the wall velocity we compute here should be an upper bound on the velocity in this epoch [26]. This effect should be important especially when the wall velocity is much smaller than the speed of sound. In this case bubbles would expand most of the time in the background of a sound wave of another bubble. This effect may significantly enhance baryon production as argued in [26].

5 Free Particle Approximation

Let us proceed to computing the wall velocity. First we will discuss a simple limit, the case where mean free paths are enormously longer than the wall. This limit has been treated thoroughly by [5, 19] and we will only discuss it briefly to illuminate a few points about which particles provide most of the friction.

In the WKB (semi-classical) approximation particles should obey a Boltzmann equation,

$$\partial_t f + \dot{\vec{x}} \cdot \partial_{\vec{x}} f + \dot{\vec{p}} \cdot \partial_{\vec{p}} f = -C[f] \tag{25}$$

Here $\dot{\vec{p}} = -\hat{z}\partial E/\partial z = (1/2E)dm^2/dx$, $\partial_t f = +v_w\partial_z f$ (where we choose the broken phase at $z = +\infty$ so the wall moves to the left) and C[f] is the collision integral. The free particle approximation consists of dropping C[f]. Since collisions are what drive f to equilibrium, we must insert equilibrium by hand as a boundary condition for incoming particles. We will use this approximation (though we should note that some of the departure from equilibrium may reflect back onto the wall [21]). In this case the Boltzmann equations can be solved exactly,

$$f^{-1} = \exp\left(\frac{E + v_w p_z}{(1 - v_w^2)T} - \frac{\gamma v_w}{T} \left(\frac{(p_z + v_w E)^2}{1 - v_w^2} + m^2\right)^{\frac{1}{2}}\right) \pm 1, \ p_z > -\sqrt{m_0^2 - m^2}$$

$$= \exp\left(\frac{E + v_w p_z}{(1 - v_w^2)T} + \frac{\gamma v_w}{T} \left(\frac{(p_z + v_w E)^2}{1 - v_w^2} + m^2 - m_0^2\right)^{\frac{1}{2}}\right) \pm 1, \ p_z < -\sqrt{m_0^2 - m^2} \ (26)$$

Here m_0 is the mass in the broken phase and \pm is + for fermions and - for bosons. Determining $\int d^3k/((2\pi)^32E)f$, the term in Eq. (4), for this expression appears hopeless, but we can expand to lowest order in v_w , which gives

$$\int \frac{d^3p}{(2\pi)^3 2E} f_0 + v_w \int \frac{d^3p}{(2\pi)^3 2E} \frac{e^{E/T}}{(e^{E/T} \pm 1)^2} \begin{cases} \sqrt{p_z^2 + m^2} - p_z, & p_z > -\sqrt{m_0^2 - m^2} \\ -\sqrt{p_z^2 + m^2 - m_0^2} - p_z, & p_z < -\sqrt{m_o^2 - m^2} \end{cases} (27)$$

This term is independent of the momentum perpendicular to the wall, p_{\perp} ; so we can perform the integral over p_{\perp} .

$$\int \frac{d^2 p_{\perp}}{(2\pi)^2 2E} \frac{e^{E/T}}{(e^{E/T} \pm 1)^2} = \frac{f_0(\sqrt{p_z^2 + m^2})}{4\pi}$$

Integrating this expression times mm' over the wall yields the velocity dependent part of the pressure; the result agrees with the integral found by [5], who have evaluated it to order m^4 .

Let us examine the integral over p_{\perp} more carefully. For bosons, the integral is

$$\int \frac{p_{\perp} dp_{\perp}}{4\pi E} \frac{1}{4} \operatorname{csch}^2 \frac{E}{2T}$$

At small E, $\operatorname{csch}^2(E/2T) \simeq 4T^2/E^2$ and the integral has a linear small momentum divergence, cut off by $\sqrt{p_z^2 + m^2}$; the dominant contribution is infrared. The resulting integral over p_z is also linearly IR divergent, as both f and $\sqrt{p_z^2 + m^2} - p_z$ behave as 1/E above m_0 . Thus, the friction from W bosons arises primarily from very infrared $(E \sim m)$ particles. This is because the Bose distribution function has a pole at E = 0, and because a particle's contribution to the Higgs equation of motion goes as 1/E.

Fermions have much more mild infrared behavior; the integral over transverse momenta is

$$\int \frac{p_{\perp}dp_{\perp}}{4\pi E} \, \frac{1}{4} \mathrm{sech}^2 \frac{E}{2T}$$

and at small E the function $\operatorname{sech}^2(E/2T)$ behaves as 1; the integral is well behaved in the infrared, even for $\sqrt{p_z^2 + m^2} = 0$, and the dominant contribution is from particles with $p_{\perp} \sim (1-2)T$. However, the integral over p_z is small p_z divergent, though only logarithmically; so the dominant contribution from top quarks comes from particles with small transverse momenta, but thermal energies, i.e. from particles at glancing incidence. This is a combined effect of the large phase space in such particles and their long time on the wall.

Now let us examine the analysis of Dine et. al. [5]. They propose to treat the particles in a relaxation time approximation. However, they compute the particle population at a point as having come off of a sheet a fixed z away from the point of interest. A particle's lifetime then actually goes as $\tau p/p_z = \tau \sqrt{1 + (p_{\perp}/p_z)^2}$, so the relaxation time is longer for particles travelling at glancing incidence. Their result then contains a logarithmic enhancement, which can be traced to these glancing incidence particles.

We will now show that no such log occurs in a relaxation time approximation when the relaxation time is short compared to the thickness of the wall. Writing $f = f_0 + \delta f$ and working to lowest order in δf , and treating the wall as stationary so $\delta f = \delta f(z + v_w t)$, the Boltzmann equations become

$$(v_w + \frac{p_z}{E})\delta f' + C[f] = v_w \frac{(m^2)'}{2E} \frac{\exp(E/T)}{(\exp(E/T) \pm 1)^2}$$
(28)

The relaxation time approximation is $C[f] = \delta f/\tau$, with τ independent of momentum. If $\tau \ll L$ (with L the wall thickness) then to lowest order in τ/L the derivative term may be dropped, giving

$$\delta f = \tau v_w \frac{(m^2)'}{2E} \frac{\exp(E/T)}{(\exp(E/T) \pm 1)^2}$$
 (29)

The friction on the wall from one species in the relaxation time approximation is then

$$\int_{-\infty}^{\infty} dz \phi' \frac{dm^2}{d\phi} \int \frac{d^3k}{(2\pi)^3 2E} \tau v_w \frac{(m^2)'}{2E} \frac{\exp(E/T)}{(\exp(E/T) \pm 1)^2}$$
(30)

which, at lowest order in an expansion in m, integrates to

$$\frac{\tau v_w}{4\pi^2} \int m^2 (m')^2 dz \,, \quad \text{(fermions)} \qquad \frac{\tau v_w}{8\pi} \int m(m')^2 dz \,, \quad \text{(bosons)}$$
 (31)

which for a tanh wall shape give $\tau v_w m_0^4/40\pi^2 L$ and $\tau v_w m_0^3/48\pi L$ respectively. The top quark contribution is isotropic, dominated by thermal particles, and has no log. The log will be recovered when $\tau >> L$ and the derivative terms in Eq. (28) become important.

We do not expect this approximation to be very good; in particular we should include the derivative terms and model C[f] more accurately. This is the goal of the remainder of the paper.

6 Fluid Approximation

In this section we will present a method for calculating the deviation from equilibrium population density δf in (4) in the presence of a moving wall. Our starting point is the Boltzmann equation,

$$d_t f \equiv \partial_t f + \dot{z} \partial_z f + \dot{p}_z \partial_{p_z} f = -C[f] \tag{32}$$

where C[f] represents the scattering integral, $E=(p^2+m^2)^{1/2}$ is the particle energy, and

$$\dot{z} = v_z = \frac{\partial}{\partial p_z} E = \frac{p_z}{E}, \qquad \dot{p}_z = -\frac{\partial}{\partial z} E = -\frac{(m^2)'}{2E}$$
 (33)

are the velocity and the force on the particle, respectively. The Boltzmann equation is the semi-classical approximation to the quantum Louville equation. To be valid the background field must vary slowly enough that particles satisfy the WKB condition:

$$p >> \frac{1}{L_w}$$

Since we expect rather thick wall, $L_w >> 1/T$, this relation is satisfied in abundance for all but the most infrared particles. We will assume that very infrared W bosons are scattered up to energies O(gT) quite readily, so W bosons with $E \sim gT$ or larger are responsible for more friction than very infrared W bosons. We will use this assumption again and again in what follows. It may be wrong³, in which case we need to extend our analysis with a special treatment of very infrared bosons. This extension must model the dynamics of the strongly coupled infrared sector of the thermal field theory, which we are not able to do at this time. We will also neglect any friction from the condensate responsible for A_F (if such a condensate exists) for similar reasons. It is our belief that this problem and the problem of determining the friction arising from thermal and O(gT) particles may be treated independently, so our analysis may be simply extended once the infrared sector is understood.

The Boltzmann treatment also requires that scatterings with the plasma are not too frequent so that particles can be to a good approximation considered on-shell for all times. To quantify this we write the Heisenberg energy-time relation $\Delta E \sim \gamma$

³The analysis of [19], which neglects transport but attempts to treat the energy dependence of δf more carefully, apparently supports our assumption, but their analysis neglects thermal corrections to the infrared boson propagator.

where γ is the appropriate damping rate which is of order g^2T [33]. Since we can only treat particles with $E, p \geq gT$ this uncertainty can be ignored.

The Boltzmann equations are nonlinear partial integro-differential relations and as such are analytically intractable. To evade this difficulty we will model each distribution function with a several parameter Ansatz called the fluid approximation. The Boltzmann equations will then yield a set of ordinary differential equations for the parameters which will be tractable analytically. The Ansatz is $f^{-1} =$ $\exp(E/T - E\delta T/T^2 - \mu/T - p_z v/T) \pm 1$, the form for a perfect fluid. We should use different parameters for each species in the plasma, but we will make an additional approximation that all light degrees of freedom (that is, all but top quarks, W bosons, and Higgs bosons) are in equilibrium at a common (space dependent) temperature $T + \delta T_{bg}$ and velocity v_{bg} . We will also give tops and anti-tops of both helicity the same distribution function. In the Minimal Standard Model this is reasonable as there is almost no CP violation, and the difference in transport properties arises only at the subleading level of weak scatterings. In two doublet models we might need to be more careful. Similarly, we will treat W bosons and Z bosons as a single species (henceforth "W bosons") whose mass squared is a weighted average of the mass squared for the W and the Z. This ensures that the effective potential parameter D is correct.

For the heavy degrees of freedom we take the distribution function to be

$$f = f_0(E + \delta) = \frac{1}{e^{(E+\delta)/T} \pm 1}, \quad \delta = -\left[\mu + \mu_{bg} + \frac{E}{T}(\delta T + \delta T_{bg}) + p_z(v + v_{bg})\right]$$
(34)

We track three perturbations with respect to the background; chemical potential μ , temperature δT and velocity v. This Ansatz is a truncation of an expansion in powers of momentum; it gives a reasonable description for the thermal particles' populations when the wall background varies slowly on the scale of the diffusion length. For top quarks this should be sufficient as the diffusion length is short and the influence of infrared particles is phase space suppressed. We discuss its validity at some length in Appendix B: suffice it to say that it appears quite reasonable for top quarks, and quite naive for W bosons.

We now outline the main steps in the derivation of the fluid equations. First we expand $d_t f$ to linear order in perturbations

$$Td_{t}f = \left[\dot{E} + d_{t}\delta\right]f'_{0}, \qquad f'_{0} = -\frac{\exp(E/T)}{(\exp(E/T) \pm 1)^{2}}$$

$$d_{t}\delta = -\left(\partial_{t} + \frac{p_{z}}{E}\partial_{z}\right)\left[\mu + \mu_{bg} + p_{z}(v + v_{bg})\right] - \frac{E}{T}\left(\partial_{t} + \frac{p_{z}}{E}\partial_{z}\right)\left(\delta T + \delta T_{bg}\right)(35)$$

This equation is written in the fluid frame so that a particle's energy is not conserved in the presence of a moving wall. The term which perturbs the population densities away from equilibrium is

$$\partial_t E f_0' = \frac{\partial_t m^2}{2E} f_0' \tag{36}$$

Note that this term is proportional to m^2 . This is the reason it is sensible to expand to linear order in perturbations. First note that $m \ll T$. For thermal particles

with $E \simeq T$, $-f'_0 \simeq f_0$ and the source for $\delta f/f$ is $O(m^2/ET)$ which is small. For infrared fermions, $-f'_0 \simeq f_0/2$ and the source is $O(m^2/ET)$ which is also small. For infrared bosons the situation is a little less rosy; at small energy $-f'_0 \simeq f_0 T/E$ and the perturbation is $O(m^2/E^2)$. Again, we will assume that these particles are scattered efficiently and postpone a more careful treatment.

The Boltzmann equations have now become

$$(-f_0')\left(\frac{p_z}{E}[\partial_z(\mu+\mu_{bg}) + \frac{E}{T}\partial_z(\delta T + \delta T_{bg}) + p_z\partial_z(v+v_{bg})] + \partial_t(\mu+\mu_{bg}) + \frac{E}{T}\partial_t(\delta T + \delta T_{bg}) + p_z\partial_t(v+v_{bg})\right) + C(\mu,\delta T,v) = (-f_0')\frac{\partial_t(m^2)}{2E}$$
(37)

The collision term depends on the deviations of all particle species from the common background temperature and velocity. We discuss it in some detail in Appendix A.

The three parameters are determined uniquely by taking three integrals of the Boltzmann equation; since our perturbations are Lagrange multipliers for particle number, energy, and momentum, the appropriate choice is $\int d^3p/(2\pi)^3$, $\int E d^3p/(2\pi)^3$, and $\int p_z d^3p/(2\pi)^3$. The resulting equations are

$$c_{2}\partial_{t}(\mu + \mu_{bg}) + c_{3}\partial_{t}(\delta T + \delta T_{bg}) + \frac{c_{3}T}{3}\partial_{z}(v + v_{bg}) + \int \frac{d^{3}p}{(2\pi)^{3}T^{2}}C[f] = \frac{c_{1}}{2T}\partial_{t}m^{2}$$

$$c_{3}\partial_{t}(\mu + \mu_{bg}) + c_{4}\partial_{t}(\delta T + \delta T_{bg}) + \frac{c_{4}T}{3}\partial_{z}(v + v_{bg}) + \int \frac{Ed^{3}p}{(2\pi)^{3}T^{3}}C[f] = \frac{c_{2}}{2T}\partial_{t}m^{2}$$

$$\frac{c_{3}}{3}\partial_{z}(\mu + \mu_{bg}) + \frac{c_{4}}{3}\partial_{t}(\delta T + \delta T_{bg}) + \frac{c_{4}T}{3}\partial_{t}(v + v_{bg}) + \int \frac{p_{z}d^{3}p}{(2\pi)^{3}T^{3}}C[f] = 0$$
 (38)

The constants c_i are defined by

$$c_i T^{i+1} \equiv \int E^{i-2} (-f_0') \frac{d^3 p}{(2\pi)^3}$$

For fermions they are $c_{1f} = \ln 2/2\pi^2$, $c_{if} = (1-2^{1-i})i!\zeta_i/2\pi^2$, i > 1. For bosons they are $c_{1b} = \ln(2/m)/2\pi^2$, $c_{ib} = i!\zeta_i/2\pi^2$. Here and throughout ζ_i is the Riemann zeta function evaluated at i. We have worked to lowest order in m/T here, but only c_{1b} and c_{2b} possess O(m/T) corrections, and these are small.

For a stationary wall all quantities are functions of $x = z + v_w t$ and the stationary fluid equations are obtained by a simple substitution

$$\partial_t \delta_i \to v_w \delta_i', \qquad \partial_z \delta_i \to \delta_i'$$
 (39)

The collision integral $\int C[f]$ depends on μ , δT , and v of all heavy species, which couples the fluid equations. However, for the top quarks the collisions which contribute to order α_s^2 arise only from collisions with light quarks and gluons, and for W bosons the contributions at order $\alpha_s \alpha_w$ and α_w^2 are primarily with light quarks (the top quark making up only 1/6 of the population of quarks). Hence it is reasonable to ignore direct collisions between top quarks and W bosons. If we included them then

the problem would become more complex, as these interactions mix top and bottom quarks, and distinguish between top helicities. To treat them properly we would need to introduce separate fluid equations for left handed bottom quarks and for each top quark handedness. Because the effect is $\sim 10\%$, we will neglect it and treat all W boson collisions with quarks as being with light quarks.

The Higgs boson interacts predominantly with the top quark via its Yukawa coupling, but since this interaction is quite efficient $(O(\alpha_t \alpha_s \ln 1/\alpha_s))$ and the Higgs has only one degree of freedom (and is lighter than the W boson if the phase transition is to be strong enough for baryon number to be conserved after its completion) we will ignore Higgs particles altogether. Hence the collision terms in the fluid equations may be treated as arising entirely through interactions with the background of light particles.

We have computed the collision integrals appearing in (38), including all diagrams which contribute to order $\alpha_s^2 \ln 1/\alpha_s$ for top quarks and to order $\alpha_w^2 \ln 1/\alpha_w$ for W bosons, in Appendix A. All diagrams are evaluated in the *leading-log* approximation. This means that only t-channel processes (which are logarithmically divergent in the limit of the zero exchange particle mass) are calculated. The result for top quarks is

$$\int \frac{d^3p}{(2\pi)^3 T^2} C[f] = \mu \Gamma_{\mu 1f} + \delta T \Gamma_{T1f} \qquad \Gamma_{\mu 1f} = .00899T \qquad \Gamma_{T1f} = .01752T$$

$$\int \frac{d^3p}{(2\pi)^3 T^3} EC[f] = \mu \Gamma_{\mu 2f} + \delta T \Gamma_{T2f} \qquad \Gamma_{\mu 2f} = .01752T \qquad \Gamma_{T2f} = .07172T$$

$$\int \frac{d^3p}{(2\pi)^3 T^3} p_z C[f] = v T \Gamma_{vf} \qquad \Gamma_{vf} = .03765T \quad (40)$$

We use the subscript f (fermion) for top quarks and b (boson) for W bosons, but we suppress them when no confusion will occur.

For W bosons we get

$$\int \frac{d^3p}{(2\pi)^3 T^2} C[f] = \mu \Gamma_{\mu 1b} + \delta T \Gamma_{T1b} \qquad \Gamma_{\mu 1b} = .00521T \qquad \Gamma_{T1b} = .01012T$$

$$\int \frac{d^3p}{(2\pi)^3 T^3} EC[f] = \mu \Gamma_{\mu 2b} + \delta T \Gamma_{T2b} \qquad \Gamma_{\mu 2b} = .01012T \qquad \Gamma_{T2b} = .03686T$$

$$\int \frac{d^3p}{(2\pi)^3 T^3} p_z C[f] = v T \Gamma_{vb} \qquad \Gamma_{vb} = .01614T \qquad (41)$$

The fluid equations then become

$$v_{w}c_{2}(\mu' + \mu'_{bg}) + v_{w}c_{3}(\delta T' + \delta T'_{bg}) + \frac{c_{3}T}{3}(v' + v'_{bg}) + \mu\Gamma_{\mu 1} + \delta T\Gamma_{T1} = \frac{v_{w}c_{1}}{2T}(m^{2})'$$

$$v_{w}c_{3}(\mu' + \mu'_{bg}) + v_{w}c_{4}(\delta T' + \delta T'_{bg}) + \frac{c_{4}T}{3}(v' + v'_{bg}) + \mu\Gamma_{\mu 2} + \delta T\Gamma_{T2} = \frac{v_{w}c_{2}}{2T}(m^{2})'$$

$$\frac{c_{3}}{3}(\mu' + \mu'_{bg}) + \frac{c_{4}}{3}(\delta T' + \delta T'_{bg}) + \frac{v_{w}c_{4}T}{3}(v' + v'_{bg}) + vT\Gamma_{v} = 0$$
(42)

where for top quarks one should use c_f and Γ_f and for W bosons one should use c_b and Γ_b .

We caution the reader not to interpret the Γ simply as rates for processes, without including the coefficients which appear in the derivative terms of the fluid equations. For instance, the rate at which a chemical potential for top quarks decays is not $\Gamma_{\mu 1f} \sim T/110$, but roughly $\sim \Gamma_{\mu 1f}/c_{2f} \sim T/9$, corresponding to a typical lifetime for a top quark before it annihilates with an anti-top of 18/T (the factor of two is because each annihilation destroys two top type particles). Similarly, the time it takes for successive small angle collisions to randomize a particle's velocity is roughly $c_4/3\Gamma_v \simeq 10/T$ for top quarks.

Collisions between massive species and light species appear in the fluid equations of the light species with opposite sign. Since the light species are treated as being at a common temperature and velocity, no $\delta T_{bg}\Gamma_T$ or $v_{bg}\Gamma_v$ appears (see Appendix A). (If we treated the background species separately, terms order $\alpha_s^2 \ln 1/\alpha_s$ would damp the difference between background species temperatures, velocities, and chemical potentials, efficiently forcing them to equal.) The background chemical potential is damped, but only by inelastic processes which enter at $O(\alpha_s^3 \ln 1/\alpha_s)$. The background fluid equations are

$$\sum c_{2}v_{w}\mu'_{bg} + \sum c_{3}(v_{w}\delta T'_{bg} + \frac{Tv'_{bg}}{3}) + N_{bg}\Gamma_{\mu bg}\mu_{bg} =$$

$$N_{t}(\mu_{f}\Gamma_{\mu 1f} + \delta T_{f}\Gamma_{T1f}) + N_{W}(\mu_{b}\Gamma_{\mu 1b} + \delta T_{b}\Gamma_{T1b})$$

$$\sum c_{3}v_{w}\mu'_{bg} + \sum c_{4}(v_{w}\delta T'_{bg} + \frac{Tv'_{bg}}{3}) =$$

$$N_{t}(\mu_{f}\Gamma_{\mu 2f} + \delta T_{f}\Gamma_{T2f}) + N_{W}(\mu_{b}\Gamma_{\mu 2b} + \delta T_{b}\Gamma_{T2b})$$

$$\frac{\sum c_{3}}{3}\mu'_{bg} + \frac{\sum c_{4}}{3}(\delta T'_{bg} + v_{w}Tv'_{bg}) = N_{t}v_{f}T\Gamma_{vf} + N_{W}v_{b}T\Gamma_{vb}(43)$$

which simply state that the particle number, energy, and momentum lost to the massive species via collisions are taken up by the light species. Here $\sum c_4 = 78c_{4f} + 19c_{4b} = (87.25)4\pi^2/30$, which is the heat capacity of the light degrees of freedom, and $N_t = 12$ and $N_W = 9$ are the number of degrees of freedom of top quarks and W bosons. The collision rate $\Gamma_{\mu bg}$ is the average over all background species of the particle number destruction rate.

Let us estimate the importance of μ_{bg} ; consider a very thick wall so that all derivatives may be dropped, and for simplicity ignore W bosons and δT and v. Then there are two fluid equations to consider,

$$N_{bg}\Gamma_{\mu bg}\mu_{bg} = N_t\mu_t\Gamma_{\mu 1} \qquad \Gamma_{\mu 1}\mu_t = v_w \frac{c_1}{2T}(m^2)'$$

The friction on the wall depends on the chemical potential of the top quark, which is $\mu_t + \mu_{bq}$. In this approximation, it is

$$v_w \frac{c_1}{2T} (m^2)' \left(\frac{1}{\Gamma_{\mu 1f}} + \frac{N_t}{N_{bg} \Gamma_{\mu bg}} \right)$$

We see that μ_{bg} is important when $N_t\Gamma_{\mu 1} > N_{bg}\Gamma_{\mu bg}$, or when the total rate at which background particles convert into top quarks exceeds the total rate at which they

annihilate via inelastic processes. If these inelastic processes were very inefficient, the friction on the wall could be significantly enhanced. Unfortunately it is quite hard to compute $\Gamma_{\mu bg}$, as there are many diagrams, all with 5 particles. The diagrams involving several gluons interfere and are not separately gauge invariant. While the diagrams are at a high perturbative order, they gain infrared log enhancements when there is a t channel exchange and one incoming gluon is soft. The diagrams involving gluons have very large color factors because the gluons are in the adjoint representation, and Bose statistics also make these diagrams large. We have made a crude estimate of these rates and find that $N_{bg}\Gamma_{bg}$ is significantly larger than $N_t\Gamma_{\mu 1f}$, so we will neglect the background species chemical potential in what follows. (This conclusion sounds like an invalidation of the perturbative expansion in α_s , but this is not so: N_{bg} is several times larger than N_t , and this makes up for the diagrams being at a higher perturbative order.)

In this approximation the background fluid equations become rather simple

$$\sum c_4(v_w \delta T'_{bg} + \frac{Tv'_{bg}}{3}) = N_t(\mu_f \Gamma_{\mu 2f} + \delta T_f \Gamma_{T2f}) + N_W(\mu_b \Gamma_{\mu 2b} + \delta T_b \Gamma_{T2b})$$

$$\frac{\sum c_4}{3} (\delta T'_{bg} + v_w T v'_{bg}) = N_t v_f T \Gamma_{vf} + N_W v_b T \Gamma_{vb}, \qquad \mu_{bg} = 0$$
(44)

Integrating these expressions, together with Eq. (42), reproduces Eq. (21). The derivative term on the lefthand side is exactly what appears in the fluid equations for the perturbed species, which allows us to eliminate the background perturbations in the fluid equations by direct substitution. The final form of the fluid equations for the top quarks is

$$v_{w}c_{2f}\mu'_{f} + v_{w}c_{3f}\partial T'_{f} + \frac{c_{3f}T}{3}v'_{f} + \mu_{f}\Gamma_{\mu 1ff} + \delta T_{f}\Gamma_{T1ff} + \mu_{b}\Gamma_{\mu 1fb} + \delta T_{b}\Gamma_{T1fb} = F_{1f}$$

$$v_{w}c_{3f}\mu'_{f} + v_{w}c_{4f}\partial T'_{f} + \frac{c_{4f}T}{3}v'_{f} + \mu_{f}\Gamma_{\mu 2ff} + \delta T_{f}\Gamma_{T2ff} + \mu_{b}\Gamma_{\mu 2fb} + \delta T_{b}\Gamma_{T2fb} = F_{2f}$$

$$\frac{c_{3f}}{3}\mu'_{f} + \frac{c_{4f}}{3}\delta T'_{f} + \frac{v_{w}c_{4f}T}{3}v'_{f} + v_{f}T\Gamma_{vff} + v_{b}T\Gamma_{vfb} = 0 \quad (45)$$

where

$$F_{1f} = \frac{v_w c_{1f}}{2} (m_t^2)' \qquad F_{2f} = \frac{v_w c_{2f}}{2} (m_t^2)'$$

$$\Gamma_{\mu 1ff} = \Gamma_{\mu 1f} + \frac{N_t c_{3f}}{\sum c_4} \Gamma_{\mu 2f} \qquad \Gamma_{T1ff} = \Gamma_{T1f} + \frac{N_t c_{3f}}{\sum c_4} \Gamma_{T2f}$$

$$\Gamma_{\mu 2ff} = (1 + \frac{N_t c_{4f}}{\sum c_4}) \Gamma_{\mu 2f} \qquad \Gamma_{T2ff} = (1 + \frac{N_t c_{4f}}{\sum c_4}) \Gamma_{T2f}$$

$$\Gamma_{\mu 1fb} = \frac{N_W c_{3f}}{\sum c_4} \Gamma_{\mu 2b} \qquad \Gamma_{T1fb} = \frac{N_W c_{3f}}{\sum c_4} \Gamma_{T2b}$$

$$\Gamma_{\mu 2fb} = \frac{N_W c_{4f}}{\sum c_4} \Gamma_{\mu 2b} \qquad \Gamma_{T2fb} = \frac{N_W c_{4f}}{\sum c_4} \Gamma_{T2b}$$

$$\Gamma_{vff} = (1 + \frac{N_t c_{4f}}{\sum c_4}) \Gamma_{vf} \qquad \Gamma_{vfb} = \frac{N_w c_{4f}}{\sum c_4} \Gamma_{vb}$$

The W fluid equations look the same with the replacements $b \leftrightarrow f$, $N_W \leftrightarrow N_t$. The collision terms have become (weakly) coupled between the heavy species, now indirectly through their influence on the background.

We also extract the behavior of the background temperature for future use:

$$\delta T'_{bg} = \frac{N_t(\mu_f \Gamma_{\mu 2f} + \delta T_f \Gamma_{T2f}) + N_W(\mu_b \Gamma_{\mu 2b} + \delta T_b \Gamma_{T2b})}{\sum c_4 (1/3 - v_w^3)}$$
(46)

We see that the resistance to the wall's movement from the heating of the plasma becomes important as the wall approaches the speed of sound. The divergent behavior at the speed of sound signifies the breakdown of our linearization of perturbations.

7 Delta function response

In order to gain some intuition for the fluid equations we study the response to a delta function source. Consider the fluid equations for the top quark, ignoring for the moment the change in the background so there is no coupling to the W boson. We can write the fluid equations in a matrix form,

$$A\delta' + \Gamma\delta = F \tag{47}$$

where

$$\delta = \begin{pmatrix} \mu \\ \delta T \\ v \end{pmatrix}, \qquad F = \begin{pmatrix} F_1 \\ F_2 \\ 0 \end{pmatrix}$$

$$V = \begin{pmatrix} c_2 v_w & c_3 v_w & \frac{c_3}{3} \\ c_3 v_w & c_4 v_w & \frac{c_4}{3} \\ \frac{c_3}{3} & \frac{c_4}{3} & \frac{c_4 v_w}{3} \end{pmatrix}, \qquad \Gamma = \begin{pmatrix} \Gamma_{\mu 1} & \Gamma_{T1} & 0 \\ \Gamma_{\mu 2} & \Gamma_{T2} & 0 \\ 0 & 0 & \Gamma_v \end{pmatrix}$$

Since the fluid equation is linear it suffices to study the solution when the source is a delta function times some column vector F. To solve this we need the homogeneous solution,

$$\delta = \sum_{i} \alpha_{i} \chi_{i} \exp(-\lambda_{i} x) \qquad x = z + v_{w} t$$

where α_i are coefficients, λ_i are the solutions to

$$Det[-A\lambda + \Gamma] = 0 \tag{48}$$

and χ_i is the vector annihilated by $-\lambda_i A + \Gamma$.

To solve the problem with a delta function source, we write a general solution to the homogeneous equations on each side of the source and apply boundary and matching conditions. Because δ should go to 0 at large distances, only the positive values of λ can have nonzero coefficients in front of the source and only the negative values can have nonzero coefficients behind. We write

$$\delta = \begin{cases} \sum_{\lambda_i > 0} \alpha_i \chi_i \exp{-\lambda x} & x > 0\\ \sum_{\lambda_i < 0} \alpha_i \chi_i \exp{-\lambda x} & x < 0 \end{cases}$$
 (49)

and determine α_i from $A\delta(0^+) - A\delta(0^-) = F$, the matching condition across the delta function. This gives

$$\sum_{i} \operatorname{sign}(\lambda_i) \alpha_i A \chi_i = F \tag{50}$$

which is solved by expanding $A^{-1}F$ in the eigenvalues χ .

We see that the solution consists of several tails, some in front of the source and some behind it. These tails model the transport of the perturbation around the source due to particle flow.

It is interesting to know how far the particles spread and how asymmetric the spreading is, so we will very briefly investigate the roots to Eq. (48). This equation is a polynomial in λ . The coefficients are very messy, but much of what we want to know is in the coefficient for λ^3 ,

$$\frac{c_4 v_w}{3} (\frac{1}{3} - v_w^2) (c_2 c_4 - c_3^2)$$

and the coefficient for λ^0 ,

$$\Gamma_v(\Gamma_{\mu 1}\Gamma_{T2} - \Gamma_{\mu 2}\Gamma_{T1})$$

Their ratio gives the product of the λ 's, and its sign tells us how many of the tails precede the source and how many follow it, as a function of v_w . We immediately see that, for a subsonic wall, one tail precedes the source and two follow it; but the sign of the coefficient for λ^3 changes at $v_w = v_s = 1/\sqrt{3}$, and all three roots then trail the source. No diffusion occurs in front of a supersonic wall, at least within the fluid approximation. It is thus quite important to the study of baryogenesis to know whether the bubble wall is subsonic or supersonic.

We will also comment that, in the special case that $v_w = 0$ and the particle decay rate is very much slower than the scattering rate (so $\Gamma_{T2}, \Gamma_v >> \Gamma_{\mu 1}, \Gamma_{T1}, \Gamma_{\mu 2}$), the root equation for λ simplifies; it is approximately

$$-\frac{c_3^2}{9}\Gamma_{T2}\lambda^2 + \Gamma_v\Gamma_{T2}\Gamma_{\mu 1} = 0$$

with roots $\lambda \to \infty$ (a non-propagating disturbance) and $\lambda^2 = 9\Gamma_v\Gamma_{\mu 1}/c_3^2$, which are decay tails. The length of the tail is $c_3/(3\sqrt{\Gamma_v\Gamma_{\mu 1}})$. By finding the small v_w limit of the coefficient for λ^1 and comparing the tails to the result of the diffusion equation we find that the diffusion length is $D = c_3^2/(9c_2\Gamma_v)$ [16], which for our value of Γ_v is D = 2.7/T for top quarks and D = 5.5/T for W bosons.

From the collision rates presented in the last section, we find the length of the tails at $v_w = 0$ is 7.4/T for top quarks and 18/T for W bosons. Top quarks do not spread very far, but W bosons do. However, both lengths are larger than the diffusion lengths of the species, so the journey is a random walk and not a free flight.

8 Wall Velocity with a Wall Shape Ansatz

In the fluid approximation the equation of motion of the Higgs field, Eq. (4), becomes

$$-(1-v_w^2)\phi'' + V_T'(\phi, T) + \frac{N_t T}{2} \frac{dm_t^2}{d\phi} (c_{1f}\mu_f + c_{2f}\delta T_f) + \frac{N_W T}{2} \frac{dm_W^2}{d\phi} (c_{1b}\mu_b + c_{2b}\delta T_b) = 0$$
(51)

This, together with the fluid equations and the equation for the background temperature, constitute a well posed set of equations for the shape of the wall. They are velocity dependent; we expect them to have a solution at a discrete set of velocities (hopefully one). However, they are nonlinear, so their solution must be numerical. For starters it would be useful to see how much progress we can make analytically. We have done so in an earlier paper [22]; here we will improve that analysis by including the background temperature.

Let us restrict the shape of the wall to an *Ansatz*,

$$\phi(z,t) = \frac{\phi_0}{2} \left(1 + \tanh \frac{z + v_w t}{L} \right) \tag{52}$$

where v_w and L are parameters to be optimized. If Eq. (51) were derived from a free energy F we would know how to proceed: we would solve $\partial F/\partial L = \int \text{Eq.}(51)\partial\phi/\partial L = 0$ and $\partial F/\partial v_w = \int \text{Eq.}(51)\partial\phi/\partial v_w = 0$ simultaneously. Since our equation of motion is dissipative, there is no free energy which generates it; however, these constraints still have the right physical content. Noting that $\partial\phi/\partial L = -(z + v_w t)\phi'/L$ and $\partial\phi/\partial v_w = t\phi'$, we guess that a good pair of constraints should be

$$\int (\text{Eq.51})\phi' dz = 0 \qquad \int (\text{Eq.51})\frac{z}{L}\phi' dz = 0 \tag{53}$$

Indeed, these have sensible physical interpretations. From Eq. (2), we see that the first of these constraints is that the total pressure on the wall should be zero; if the total pressure were nonzero then the wall would accelerate, changing v_w . The second equation is an asymmetry in the total pressure between the front and back of the wall. If it were not zero there would be a net compressive or stretching force on the wall, changing L.

Next we must deal with the variation of temperature across the wall. Write the temperature in the broken phase as T (which is T_a in the language of section 4) and the temperature at a position z as $T(z) = T + \delta T_{bg}(z)$. We will solve for δT_{bg} using Eq. (46) and the boundary condition $\delta T_{bg}(z \to \infty) = 0$ and correct (51) to linear order in δT_{bg} . The correction is $\delta T_{bg}dV'_T/dT \simeq 4D\phi T\delta T_{bg}$.

The integrals (53) for the constant temperature, equilibrium part of (51) can be performed; they give

$$\int (\Box \phi + V_T'(\phi))\phi' = V_T(\phi_0) - V_T(0) \equiv -\Delta V_T$$
(54)

$$\int [\Box \phi + V_T'(\phi)] \frac{z}{L} \phi' = \frac{(1 - v_w^2)\phi_0^2}{6L^2} - \frac{1}{2} [\Delta V_T + \Xi]$$
 (55)

$$\Xi \equiv C\phi_0^2(\zeta_2 - 1)T^2 + \frac{E\phi_0^3 T}{2} - \frac{5\lambda_T \phi_0^4}{24} + \frac{A_f g_w^6 T^4}{12} \left(2.79 + \frac{1}{2} \ln \frac{\phi_0}{T}\right)$$
 (56)

Note that the $\Box \phi$ term acts to stretch the wall (increase L) while V_T acts to accelerate and compress the wall. The coefficient 2.79 in the last term is the only place where our choice for the function Pit enters our computation.

Next we must evaluate the integrals

$$4DT \int \delta T_{bg} \phi \phi' dz$$
, $4DT \int \delta T_{bg} \frac{z}{L} \phi \phi' dz$

for the background temperature,

$$\int N_t(c_{1f}\mu_f + c_{2f}\delta T_f) \frac{y^2}{2} \phi \phi'(z) dz , \quad \int N_t(c_{1f}\mu_f + c_{2f}\delta T_f) \frac{y^2}{2} \frac{z}{L} \phi \phi'(z) dz$$

for quarks, and similarly for W bosons; to do this we Fourier transform the integrals to

$$\int N_t(c_{1f}\widetilde{\mu}_f(k) + c_{2f}\widetilde{\delta T}_f(k)) \frac{y^2}{2} \widetilde{\phi \phi'}(-k) \frac{dk}{2\pi}$$

et cetera. One complication is that c_{1b} is weakly z dependent; we approximate it at its value where $\phi \phi'$ is maximum. Evaluating $\widetilde{\phi} \phi'$ by a contour integration, we find

$$\widetilde{\phi\phi'}(k) = \frac{\phi_0^2}{2} (1 - ikL/2) \frac{kL\pi}{2} \operatorname{csch} \frac{kL\pi}{2} \qquad \frac{\widetilde{z\phi\phi'}(k)}{L} = i \frac{d\widetilde{\phi\phi'}}{d(kL)}$$
 (57)

We determine $\tilde{\mu}$ and δT from the fluid equations; they can be written in a matrix form by writing $\delta = [\mu_f, \delta T_f, v_f, \mu_b, \delta T_b, v_b]^T$; the fluid equations become

$$A_{ij}\delta'_j + \Gamma_{ij}\delta_j = F_i\phi\phi' \qquad \delta T'_{bg} = R_i\delta_i \tag{58}$$

The coefficient matrices A and Γ and the source vector F can be read off from Eq. (45), and the form of R can be read off from Eq. (46).

 F_i has one term $\sim c_{1b}$ which is weakly position dependent; again we approximate it as its value where $\phi \phi'$ is maximum. The fluid equations are then easy to Fourier transform, becoming

$$ik\tilde{\delta}_i + (A^{-1})_{ij}\Gamma_{jk}\tilde{\delta}_k = (A^{-1})_{ij}F_j\widetilde{\phi}\phi' \qquad ik\tilde{\delta}T_{bg} = R_i\tilde{\delta}_i$$
 (59)

Now denote the eigenvalues of $(A^{-1}\Gamma)$ as λ_i , and write the matrix whose columns are the eigenvectors of $(A^{-1}\Gamma)$ as χ , so that

$$(A^{-1}\Gamma)_{ij}\chi_{jk} = \chi_{ik}\lambda_k$$

(with no sum on k). Also define $\alpha_i = (\chi^{-1})_{ij}\delta_j$ and $S_i = (\chi^{-1})_{ij}(A^{-1}F)_j$, which are the deviation from equilibrium and the source in the basis of eigenvectors. Multiplying the fluid equations on the left by χ^{-1} , we find

$$\tilde{\alpha}_i = \frac{S_i}{\lambda_i + ik} \widetilde{\phi} \widetilde{\phi}'(k) \qquad ik \widetilde{\delta} \widetilde{T}_{bg} = R_i \chi_{ij} \frac{S_j}{\lambda_j + ik} \widetilde{\phi} \widetilde{\phi}'(k) \tag{60}$$

The equation for δT_{bg} only determines its value up to a constant of integration, which in Fourier space is a delta function; the coefficient of the delta function is determined by the boundary condition for δT_{bg} . We find

$$\widetilde{\delta T}_{bg} = R_i \chi_{ij} \left(\frac{S_j}{ik(\lambda_j + ik)} - \frac{S_j \pi}{\lambda_j} \delta(k) \right) \widetilde{\phi \phi'}(k)$$
 (61)

where $\delta(k)$ is the Dirac delta function.

The contributions to Eq. (53) in this notation are

$$\int \frac{dk}{2\pi} \left[f_i \chi_{ij} \frac{S_j}{\lambda_j + ik} + 4DT R_i \chi_{ij} \left(\frac{S_j}{ik(\lambda_j + ik)} - \frac{S_j \pi}{\lambda_j} \delta(k) \right) \right] \widetilde{\phi \phi'}(k) \widetilde{\phi \phi'}(-k) \tag{62}$$

and

$$\int \frac{dk}{2\pi L} \left[f_i \chi_{ij} \frac{S_j}{\lambda_j + ik} + 4DT R_i \chi_{ij} \left(\frac{S_j}{ik(\lambda_j + ik)} - \frac{S_j \pi}{\lambda_j} \delta(k) \right) \right] \widetilde{\phi \phi'}(k) \widetilde{z \phi \phi'}(-k) \quad (63)$$

The vector f above, which gives the force on the field from δ , can be read off from Eq. (51).

How does transport enter these integrals? The λ_i are the inverse lengths of exponential tails. The no transport limit is the limit in which the λ_i are large. In this limit the ik in the denominator is irrelevant. Since $\widetilde{\phi\phi'}(k)\widetilde{\phi\phi'}(-k)$ is real, the ik reduces the value of Eq. (62); transport, by spreading out the perturbation, has reduced the friction on the wall.

Eq. (62)- (63) may be solved using the following integrals:

$$\int \frac{dk}{2\pi} \frac{1}{\lambda + ik} \widetilde{\phi} \widetilde{\phi}'(k) \widetilde{\phi} \widetilde{\phi}'(-k) = \frac{\phi_0^4}{16} \left((\lambda L - \frac{(\lambda L)^3}{4}) I_1(\frac{\lambda L \pi}{2}) + \frac{\lambda L}{3} \right) (64)$$

$$\int \frac{dk}{2\pi L} \frac{1}{\lambda + ik} \widetilde{\phi} \widetilde{\phi}'(k) \widetilde{z} \widetilde{\phi} \widetilde{\phi}'(-k) = \frac{\phi_0^4}{16} \left((\frac{(\lambda L)^2}{2} + \frac{\lambda L}{2} - 1) I_1(\frac{\lambda L \pi}{2}) + (1 - \frac{(\lambda L)^2}{4}) I_2(\frac{\lambda L \pi}{2}) - \frac{1}{6} \right) (65)$$

$$\int \frac{dk}{2\pi} \frac{1}{ik(\lambda + ik)} \widetilde{\phi} \widetilde{\phi}'(k) \widetilde{\phi} \widetilde{\phi}'(-k) = \frac{-1}{\lambda} (\text{Eq.64})$$
(66)

$$\int \frac{dk}{2\pi L} \frac{1}{ik(\lambda + ik)} \widetilde{\phi}\widetilde{\phi}'(k) \widetilde{z}\widetilde{\phi}\widetilde{\phi}'(-k) = \frac{-1}{\lambda} (\text{Eq.}65) - \frac{5\phi_0^4}{96}$$
(67)

Where we have defined the integrals

$$I_1(a) = \int_{-\infty}^{+\infty} \frac{x^2 \operatorname{csch}^2 x}{x^2 + a^2} dx \qquad I_2(a) = \int_{-\infty}^{+\infty} \frac{x^3 \operatorname{csch}^2 x \operatorname{coth} x}{x^2 + a^2} dx \tag{68}$$

Evaluating these by contours gives

$$I_{1}(a) = \frac{\pi a}{\sin^{2} a} - 2 - \sum_{n=1}^{\infty} \frac{n(2\pi a)^{2}}{((n\pi)^{2} - a^{2})^{2}}$$

$$I_{2}(a) = \frac{\pi a^{2} \cos a}{\sin^{3} a} - 1 + \sum_{n=1}^{\infty} 2n\pi^{2} a^{2} \frac{3a^{2} + (n\pi)^{2}}{((n\pi)^{2} - a^{2})^{3}}$$
(69)

Numerically, these expressions suffer from cancelling divergences near $a = n\pi$. For large values of a the integrals possess useful asymptotic series

$$I_1(a) \to 4 \sum_{n=1}^{\infty} \frac{(-)^{n+1}(2n)!\zeta(2n)}{(2a)^{2n}} \qquad I_2(a) \to 2 \sum_{n=1}^{\infty} \frac{(-)^{n+1}(2n+1)!\zeta(2n)}{(2a)^{2n}}$$
 (70)

At small values of a it is useful to rearrange the infinite series into Taylor expansions,

$$I_{1}(a) = \frac{\pi a}{\sin^{2} a} - 2 - 4 \sum_{n=1}^{\infty} n \left(\frac{a}{\pi}\right)^{2n} \zeta(2n+1)$$

$$I_{2}(a) = \frac{\pi a^{2} \cos a}{\sin^{3} a} - 1 + \sum_{n=1}^{\infty} n(n+1) \left(\frac{a}{\pi}\right)^{2n} \left(\frac{3a^{3}}{\pi^{2}} \zeta(3+2n) + \zeta(1+2n)\right)$$
(71)

which have radius of convergence π .

This completes the evaluation of Eq. (53). These two constraint equations determine curves in the space of v_w , L and their intersections are self-consistent solutions for the wall shape and velocity within our $Ans\"{a}tze$ and approximations. These curves are illustrated in Figure 2.

9 Solving the Equations of Motion

It is also possible to solve (51) and the fluid equations numerically for a general wall shape. Although they constitute a nonlinear system of equations, they are linear in δ ; we can therefore solve for δ as (nonlocal) functions of ϕ and reduce the system to a single integro-differential relation for ϕ . We begin with Eq. (59), but including the position dependence of F, so we must Fourier transform $F\phi\phi'$ as a unit. Now write

$$\widetilde{S}_i \equiv (\chi^{-1})_{ij} (A^{-1})_{jk} \widetilde{F_k \phi \phi'} \tag{72}$$

We quickly find

$$\tilde{\delta}_i = \chi_{ij} \frac{\tilde{S}_j}{\lambda_j + ik} \tag{73}$$

which can be inverse transformed into a convolution,

$$\delta_i(z) = \chi_{ij} \int dy G_j(y - z) (\chi^{-1} A^{-1} F)_j(y) \phi \phi'(y)$$

$$G_j(x) \equiv \operatorname{sign}(\lambda_j) \theta(x \operatorname{sign}(\lambda_j)) \exp(-\lambda_j x)$$
(74)

Here G is the Green's function for fluid perturbations. Now given a spatial configuration for ϕ , say on a lattice of points, we may integrate numerically to find δ and integrate again to find T_{bg} . This gives us the full equation of motion (51). If the equation of motion had been derived from a free energy, then we know that changing ϕ in the direction dictated by the equation of motion reduces the free energy, and is guaranteed to approach a minimum if one exists. We may hope that evolving ϕ in the direction dictated by the equation of motion will lead us towards a solution

of the equations of motion, but we must be a little careful because there is only a solution at select values of v_w , and because the wall has a zero mode. The naive way to evolve v_w towards its correct value is to move it in the direction dictated by the total pressure on the wall, $\int (\text{Eq.51})\phi' dz$. We then subtract a quantity proportional to ϕ' from the equation of motion when we correct ϕ , as otherwise part of the correction we implement will just be a shift in the wall position. This approach should work below the speed of sound, but above the speed of sound the pressure may decrease with velocity (as the temperature elevation reduces).

We have implemented this procedure numerically, and find that the wall does approach a solution of the equation of motion for subsonic starting velocity. Since the lattice on which ϕ is defined need only be 1 dimensional (as the wall is planar) it is easy to make the stepsize small enough that the results are robust; our results agree to 0.2 % when we change stepsize from 1/T to 2/T. We find that the wall is somewhat deformed from a tanh, appearing steeper on the side facing the symmetric phase and shallower on the side facing the broken phase. Part of this is due to the two loop terms in the effective potential, but it also turns out to be true when we use just the 1 loop potential, which produces a symmetric wall at equilibrium. We can understand this deformation as follows; the source for excess particles goes as $\phi \phi'$, which peaks above $\phi = \phi_0/2$. The excess particles are on average swept further up the wall towards large ϕ because of the motion of the wall with respect to the plasma. Hence most of the frictive force on the wall occurs at large ϕ , and stretches out the upper part of the wall.

10 Results and Conclusions

The wall velocity computed from the tanh Ansatz and numerically are tabulated for several effective potential parameters in Table 1 and the wall shape they give is compared in Figure 3. We see that the Ansatz returns the velocity accurately, although at large A_F it gives a wrong wall shape. The column ϕ_0/T is the Higgs vev after the phase transition has completed, accounting for the heating of the plasma due to the release of latent heat in the transition.

There is always a subsonic solution within the approximations that we have made, because as one approaches the speed of sound from below the temperature is elevated by more and more. In all cases in the table with $A_F = 0$, the only solution is subsonic. This is because the liberated latent heat raises the temperature of the plasma, which inhibits the motion of the wall. Neglecting the background temperature, as we did in [22], produces a supersonic wall, so the effect is quite important. The result that the wall is subsonic is robust in the sense that, if we have underestimated all collision rates by a factor of two, we still find only a subsonic solution. Also note that the velocity is quite weakly dependent on the Higgs mass; in the range $0 < m_H < 90$ GeV, $.38 < v_w < .46$. Recall that this result ignores the Higgs particle contribution to friction and may underestimate the contribution of infrared W bosons, which can only make the wall velocity lower. However, top quarks were typically responsible for about 60% of the friction and 65% of the liberated latent heat, so we do not anticipate

λ_T	$m_H(T=0)$	A_F	Ansatz v_w	Ansatz L	numerical v_w	ϕ_0/T
.0204	0	0	.351	29	.365	.987
.023	34	0	.356	28	.374	.907
.03	50	0	.365	26	.392	.757
.04	70	0	.377	25	.412	.635
.05	81	0	.390	24	.428	.562
.06	91	0	.401	23	.441	.516
.03	50	.1	.481, run	18	.496	.998
.04	70	.1	.497, .97	15, 14	.513	.861
.05	81	.1	.508, .91	13, 11	.524	.777
.03	50	.2	.499, run	15	.510	1.12
.04	70	.2	.513, run	12	.524	.971
.05	81	.2	.522, .98	11, 7.7	.533	.878
.06	91	.2	.528, .96	9.6, 6.2	.539	.814
.04	70	.3	.519, run	11	.530	1.05
.05	81	.3	.527, run	9.4	.537	.952
.06	91	.3	.534, run	8.5	.543	.882
.07	98	.3	.538, run	7.8	.546	.831

Table 1: Wall velocity and thickness and Higgs vev after transition at several effective potential parameters. The second entries in the *Ansatz* velocity and length columns for some entries are detonation solutions; in some cases the *Ansatz* predicts runaway.

that infrared particles will change our results a great deal.

Including the background temperature has also reduced the dramatic stretching of the wall found in [22]. This stretching arose because the force on the wall from δf is predominantly far back on the wall. In the limit where decay rates are fast compared to the wall passage time, $\delta f \sim \phi \phi'$, which peaks well above $\phi = \phi_0/2$. The force on the wall from δf depends on $\delta f \phi \phi'$, which peaks even more strongly on the upper part of the wall. Transport compounds this effect as particles sweep up the wall because of its movement. The result is that most of the force from δf is far back on the wall, stretching it out. However, δT_{bg} is largest (for subsonic walls) in front of the wall in the symmetric phase, so it tends to exert more force on the front of the wall, which compresses it. This partially compensates the stretching we found in [22].

In all cases in the table in which $A_F \neq 0$, the Ansatz technique tells us that there is a supersonic solution; this is always very relativistic and sometimes accelerates without limit. While this result is not robust (it may be incorrect if friction from infrared particles is important), it is possible that the wall does become supersonic in these cases. However, the fluid approximation is not valid in these conditions, because the front part of the wall becomes quite thin. A more careful analysis shows that the compression of the front of the wall greatly increases the friction and prevents ultrarelativistic motion. This is discussed in Appendix C.

In conclusion, if there is a gauge boson condensate in the symmetric phase, and if

neither this condensate nor infrared bosons impart substantial friction, then the wall becomes supersonic. On the other hand, if there is no gauge boson condensate in the symmetric phase, the wall is definitely subsonic just due to friction from thermal particles and the release of latent heat.

11 Acknowledgements

We thank the Sir Isaac Newton Institute for Mathematical Sciences, Cambridge, England, for hospitality during the early part of this work. We are very grateful to Misha Shaposhnikov, Arthur Heckler, Michael Joyce and Neil Turok for enlightening conversations. We would also like to thank Marco Moriconi for reminding us how to do partial fractions. GM acknowledges support from an NSF graduate fellowship and TP support by PPARC.

12 Appendix A: Scattering Rates

In this appendix we discuss the computation of collision integrals. The collision integral appearing in the Boltzmann equation is, to second order in α ,

$$C[f] = \sum \frac{1}{2E_p} \int \frac{d^3k}{(2\pi)^9} \frac{d^3k'}{2E_k} |\mathcal{M}(s,t)|^2 (2\pi)^4 \delta^4(p+k-p'-k') \mathcal{P}[f_i]$$
(75)
$$\mathcal{P}[f_i] = f_1 f_2 (1 \pm f_3) (1 \pm f_4) - f_3 f_4 (1 \pm f_1) (1 \pm f_2)$$

where the sum is over all four leg diagrams, p refers to the incoming particle, k is the particle it hits, and p' and k' are the outgoing particles; the legs are labelled as 1, 2, 3, 4 respectively. \mathcal{M} is the scattering amplitude for the process. The f's are population factors; the positive expression represents a particle being removed from the state with momentum p by a collision and is weighted by the population of particles in that state and of the state it collides with. The negative term in $\mathcal{P}[f_i]$ accounts for particles scattering into the state. The factors $1 \pm f$ for the outgoing particles arise from particle statistics; the \pm is a - for fermions (corresponding to Pauli blocking) and a + for bosons (for stimulated emission). Weldon has given an excellent derivation of this expression from the discontinuity on the real time axis of the self-energy of the propagator [32]. Extending his technique to include gauge particles in a general covariant gauge proves to introduce difficulties. The structure of the collision integral arises from the poles of propagators in a self-energy diagram, and the propagator $D_{\mu\nu}=(g_{\mu\nu}-\xi k_{\mu}k_{\nu}/k^2)/k^2$ has extra on shell divergences for $\xi \neq 0$. Such infrared problems have been discussed by Braaten and Pisarski [33], who have shown that it is sufficient to work in the gauge $\xi = 0$.

Let us begin by analyzing the population factors. Without loss of generality we may write $f_i = 1/(\exp a_i \pm 1)$, and noting that $(1 \pm f_i) = f_i \exp a_i$ we find

$$f_1 f_2 (1 \pm f_3) (1 \pm f_4) - (1 \pm f_1) (1 \pm f_2) f_3 f_4 = (e^{a_3 + a_4} - e^{a_1 + a_2}) f_1 f_2 f_3 f_4$$

The equilibrium value of a_i is $\gamma(E_i - \vec{v} \cdot \vec{p_i})/T$ with a common \vec{v} and T for all species. In this case, C[f] = 0 by energy and momentum conservation. This holds for higher order graphs as well. In the Boltzmann approximation the collision integral is local, so it also holds for a common spatially varying temperature and velocity.

Now let $a_i = \gamma (E_i - \vec{p_i} \cdot \vec{v_{bg}}) / T_{bg} - \delta_i$, with δ_i small; then

$$\exp(a_1 + a_2) = \exp(\sum_{i} \gamma (E_i - \vec{p}_i \cdot \vec{v}) / T_{bg}) \exp(-\delta_1 - \delta_2)$$

$$\simeq \exp(\sum_{i} \gamma (E_i - \vec{p}_i \cdot \vec{v}) / T_{bg}) (1 - \delta_1 - \delta_2)$$

to linear order in δ , and hence

$$\mathcal{P}[f_i] \simeq (\sum \delta) f_1 f_2 (1 \pm f_3) (1 \pm f_4)$$

where the sum on delta is over incoming *minus* outgoing legs.

Now let us compute the $O(\alpha_s^2)$ collision rates for top quarks. All t-channel diagrams which contribute at order α_s^2 are shown in the first column of Figure 1. There are also s-channel processes. These diagrams interfere, but luckily the cross-amplitudes are all $O(m^2/T^2)$ and can be neglected. Top quarks can also decay directly, with a matrix element $O(g_w^2)$, but this process is time dilated and phase space suppressed, which reduces its importance by $O(m^2/ET)$. It therefore contributes at order $\alpha_w \alpha_y$ and can be neglected.

When we compute the cross-sections of these diagrams using free particle propagators, we find that the t-channel processes lead to logarithmic infrared divergences. At finite temperature these divergences are cut off by the interaction of the exchange particle with the plasma, so the t-channel diagrams contribute at order $\alpha_s^2 \ln 1/\alpha_s$. The exact thermal propagators are quite complicated, but if we are willing to make an error in the leading constant (but get the coefficient of the log right) we can make a simple approximation which renders the computation more tractable. For an exchanged (top) quark, the correct dispersion relation is very similar to that of a massive particle with $m_q^2 = g_s^2 T^2/6$ [34]. This correction is of order the (space dependent) contribution from the physical mass, $m_t^2 = y_t^2 \phi^2/2$, which we will therefore neglect, making the collision integral ϕ independent. For the bosons the dispersion relations are quite complex. For space-like momenta, such as occur for t-channel gluon or W boson exchange, the longitudinal components of the propagator are Deby screened, and the transverse parts Landau damped, below the plasma mass, which is $m_g^2 = 2g_s^2T^2$ for gluons and $m_W^2 = (5/3)g_w^2T^2$ for W bosons [35]. To approximate this effect we modify the denominator of the propagator, making it $t-m^2$, where m is the appropriate plasma mass of the exchange particle. This approximation is quite rough; it should yield the correct leading log coefficient, but not the correct leading constant. Hence we can only work to leading log accuracy. We therefore drop s channel processes, which do not produce logarithms, set u = -s (which is legitimate in the leading log approximation), and keep only the st/t^2 dependence of annihilation and absorption-reemission processes and the s^2/t^2 dependence of scattering processes.

We will also systematically drop terms of order m/T, which allows us to treat the outgoing lines as approximately massless. In all cases the collision rates are dominated by thermal particles, and the infrared log divergence arises primarily when the exchange momentum is between T and m, so this approximation is justified.

Top quark annihilation rates

Now we will compute a simple annihilation diagram, quarks go to gluons with matrix element (in the leading log approximation) $\simeq -(64/9)g_s^4 st/(t-m_q^2)^2$. The collision integral, integrated over $d^3p/(2\pi)^3T^2$, is

$$\frac{64g_s^4}{9} \int \frac{d^3p}{(2\pi)^3 T^3 2E_p} \frac{d^3k}{(2\pi)^3 2E_k} [2\mu + (E_p + E_k)\delta T/T + (p_z + k_z)v]
\int \frac{d^3p'}{(2\pi)^3 2E_{p'}} \frac{d^3k'}{(2\pi)^3 2E_{k'}} \frac{-st}{(t - m_q^2)^2} (2\pi)^4 \delta^4(p + k - p' - k') \mathcal{P}[f_i]$$
(76)

In the leading log approximation the energy transfer is small, so we may approximate

$$\mathcal{P} = f_p f_k (1 + f_{p'})(1 + f_{k'}) \simeq f_p f_k (1 + f_p)(1 + f_k)$$

where the 1+f use the Bose population function and the f use the Fermi population function. In this approximation, \mathcal{P} is independent of p' and k' and the integrals over p' and k' are Lorentz invariant and may be performed in the center of mass frame. The integral over k' performs the three spatial delta functions, so that $\vec{k'} = -\vec{p'}$. The integral over p', making a small mass approximation for t, is

$$\int \frac{p'^2 dp' d\Omega_{p'}}{(2\pi)^3 2E_{p'} 2E_{k'}} 2\pi \delta(2E_p - 2E_{p'}) \frac{(2p \cdot k)2pp'(1 - \cos \theta')}{(2pp'(1 - \cos \theta') + m_q^2)^2} \simeq \frac{1}{8\pi} \ln \frac{2p \cdot k}{m_q^2}$$
(77)

to leading log accuracy. We now perform the remaining integrals in the plasma frame. The argument of the log contains the only dependence on p or k; $2p \cdot k = 2|\vec{p}||\vec{k}|(1-\cos\theta) + O(m_q^2)$, with θ the plasma frame angle between \vec{p} and \vec{k} . The remaining integrals are

$$\frac{64g_s^4}{9T^3} \frac{1}{8\pi} \int \frac{p^2 dp d\Omega_p}{(2\pi)^3 2E_p} \frac{k^2 dk d\varphi d\cos\theta}{(2\pi)^3 2E_k} \left[2\mu + (E_p + E_k)\delta T/T + (p_z + k_z)v \right]
f_p f_k (1 + f_p)(1 + f_k) \ln \frac{2pk(1 - \cos\theta)}{m_q^2}$$
(78)

The integral over $(p_z + k_z)v$ vanishes when we integrate over $d\Omega_p$, although (only) it will contribute when we integrate over $p_z d^3 p/T^3$. The integral over θ gives approximately $2\ln(4pk/m_q^2)$, again dropping a constant and keeping only the leading log. The remaining angular integrals are all trivial. The energy integrals are dominated by thermal energies where we are justified in approximating $p = E_p$, and we get

$$\frac{g_s^4}{18\pi^5 T^3} \int pk[2\mu + (p+k)\delta T/T] \ln \frac{4pk}{m^2} f_p f_k (1+f_p)(1+f_k) dp dk \tag{79}$$

Using the approximation

$$\int p^n \ln \frac{p}{T} f_p(1 + f_p) dp \simeq \ln(n + 1/2) \int p^n f_p(1 + f_p) dp$$
 (80)

which is justified asymptotically and is reasonably accurate already at small values of n, we perform these integrals and get

$$\frac{8\alpha_s^2}{9\pi^3} \left(2\mu \frac{9\zeta_2^2}{16} \ln \frac{9T^2}{m_q^2} + 2\delta T \frac{3\zeta_2}{4} \frac{7\zeta_3}{4} \ln \frac{15T^2}{m_q^2} \right) T \tag{81}$$

The integrals over $E_p d^3 p$ and $p_z d^3 p$ are performed similarly and introduce no further complications.

Scattering Processes

Scattering diagrams are somewhat more complicated because the sum over chemical potentials and energies involves both incoming and outgoing particles. Consider the t channel gluon exchange diagrams. The amplitude squared and summed over outgoing states is $\simeq 40g_s^4s^2/t^2$ for a top quark scattering off a gluon and $= (5/6)32g_s^4(s^2+u^2)/t^2 \simeq (160/3)g_s^4s^2/t^2$ for a top quark scattering off a quark (when it scatters from another top quark, $\sum \delta = 0$ as the other top is at the same temperature and velocity). We have replaced $u \to -s$ which is legitimate in the leading log approximation. The sum over perturbations $\sum \delta = 0\mu + (E_p - E_{p'})\delta T + (p_z - p'_z)v$ so these diagrams do not damp chemical potential. Also, the integration measure is symmetric under $p \leftrightarrow p'$ and $k \leftrightarrow k'$, but the integrand is antisymmetric, so the diagrams do not contribute to the first fluid equation. Also, the integral $p_z d^3 p$ gets no contribution from δT because the integrand is invariant under parity transformation $\vec{p_i} \to -\vec{p_i}$, with $\vec{p_i} = \{\vec{p_i}, \vec{k_i}, \vec{p'}, \vec{k'}\}$ and the integral over $E_p d^3 p$ similarly gets no contribution from v. Hence we need only two integrals,

$$\int_{pkp'k'} \frac{A}{T^4} \frac{s^2}{(t - m_g^2)^2} (2\pi)^4 \delta(p + k - p' - k') f_p f_k (1 - f_{p'}) (1 \pm f_{k'}) \begin{cases} E_p (E_p - E_{p'}) \\ p_z (p_z - p_z') \end{cases} (82)$$

where $A=40g_s^4$ for the scattering off a gluon, and $A=(160/3)g_s^4$ for the scattering off a quark and of course the correct population densities for bosons and fermions ought to be chosen. We use the symmetry of the integration measure and $\mathcal{P}[f]$ under $p \leftrightarrow p'$ to rewrite $E_p(E_p - E_{p'}) \to (E_p - E_{p'})^2/2$ and write it in a Lorentz invariant form as $[u \cdot (p-p')]^2/2$, where u_μ is the unit vector in the time direction of the plasma frame. Similarly, $p_z(p_z - p_z') \to -t/6 + [u \cdot (p-p')]^2/6$.

Writing the center of mass frame angle between \vec{u} and \vec{p} as β , the integrals over p' and k' give, in the center of mass frame,

$$\frac{A}{8\pi} \begin{cases}
(|\vec{u}| | \vec{p} | \sin \beta)^2 \ln \frac{4p^2}{m_g^2} \\
\frac{1}{3} [(|\vec{u}| | \vec{p} | \sin \beta)^2 + 2p^2] \ln \frac{4p^2}{m_g^2}
\end{cases}$$
(83)

A quick calculation gives

$$|\vec{u}|_{cm}|\vec{p}|_{cm}\cos\beta = \vec{u}\cdot\vec{p} = u\cdot(p-k)/2 = \frac{(E_p - E_k)_{\text{plasma}}}{2}$$

and

$$|\vec{u}|_{cm}|\vec{p}|_{cm} = \frac{|\vec{p} + \vec{k}|_{\text{plasma}}}{2}$$

so, in terms of the plasma frame angle θ between \vec{p} and \vec{k} , (83) is

$$\frac{A}{16\pi} \begin{cases}
E_p E_k (1 + \cos \theta) \ln(2E_p E_k (1 - \cos \theta) / m_g^2) \\
\frac{1}{3} E_p E_k (3 - \cos \theta) \ln(2E_p E_k (1 - \cos \theta) / m_q^2)
\end{cases}$$
(84)

Recall that $A = 40g_s^4$ ($A = (160/3)g_s^4$) for scattering off a gluon (quark). We can now do the remaining integrations as above, using the same leading log approximation as in the previous section. the result is

$$\frac{5}{\pi^3} 2\zeta_2^2 \alpha_s^2 \ln \frac{25T^2}{m_g^2} T \begin{cases} 1/2 \\ 1/2 \end{cases}, \qquad \frac{20}{3\pi^3} \zeta_2^2 \alpha_s^2 \ln \frac{25T^2}{m_g^2} T \begin{cases} 1/2 \\ 1/2 \end{cases}$$
(85)

for scattering off a gluon and a quark, respectively. Bose statistics have made scattering from a gluon more important than from a quark, even though the matrix element squared is smaller.

Results for top quark diagrams

We now tabulate the contributions of the collision integrals to the decay constants Γ for the top quarks.

The contributions of two annihilation diagrams, both with matrix elements $\simeq -(64/9)st/(t-m_g^2)^2$, sum to

$$\frac{32\alpha_s^2}{9\pi^3}T \begin{cases}
(9\zeta_2^2/16)\ln(9T^2/m_q^2) & \Gamma_{\mu 1} \\
(21\zeta_2\zeta_3/16)\ln(15T^2/m_q^2) & \Gamma_{\mu 2} \\
(21\zeta_2\zeta_3/16)\ln(15T^2/m_q^2) & \Gamma_{T1} \\
(135\zeta_2\zeta_4/64)\ln(21T^2/m_q^2) + (49\zeta_3^2/32)\ln(25T^2/m_q^2) & \Gamma_{T2} \\
(45\zeta_2\zeta_4/64)\ln(21T^2/m_q^2) & \Gamma_v
\end{cases}$$
(86)

The scattering diagrams when summed yield

$$\frac{25\alpha_s^2}{3\pi^3}T \begin{cases} \zeta_2^2 \ln(25T^2/m_g^2) & \Gamma_{T2} \\ \zeta_2^2 \ln(25T^2/m_g^2) & \Gamma_v \end{cases}$$
 (87)

Absorption and re-emission of a gluon, with matrix element $\simeq -(64/9)st/(t-m_a^2)^2$, contributes

$$\frac{\alpha_s^2}{36\pi^3} T \begin{cases} 135\zeta_2\zeta_4 \ln(21T^2/m_q^2) - 98\zeta_3^2 \ln(25T^2/m_q^2) & \Gamma_{T2} \\ 90\zeta_2\zeta_4 \ln(21T^2/m_q^2) - 98\zeta_3^2/3 \ln(25T^2/m_q^2) & \Gamma_v \end{cases}$$
(88)

These collision integrals were evaluated in analogous manner to the gluon exchange scatterings; after integrating over p' and k' one obtains $(16g_s^2/9\pi)(\gamma vp\cos\beta)^2 \rightarrow (16g_s^2/9\pi)(1/4)[(p-k')\cdot u]^2$ for the contribution to δT and $(16g_s^2/27\pi)[(\gamma vp\cos\beta)^2 + p^2] \rightarrow (16g_s^2/27\pi)(1/4)\{[(p-k')\cdot u]^2 + 2p\cdot k\}$ for the contribution to v.

Evaluating (86) – (88) numerically, using $\alpha_s = 0.12$, $m_g^2 = 2g_s^2T^2$, and $m_q^2 = g_s^2T^2/6$, we find $\Gamma_{\mu 1f} = .008993T$, $\Gamma_{\mu 2f} = .01752T = T\Gamma_{T1f}$, $\Gamma_{T2f} = 0.07172T$, and $\Gamma_{vf} = 0.03765T$ [36]. By comparing the contributions from various diagrams one finds that scatterings dominate Γ_v , but Γ_{T2} arises mainly from annihilations.

We should comment that we have left out one potentially important diagram, weak flavor changing scattering, which converts left handed top quarks to bottom quarks. Because of the linear Coulomb singularity, cut off by Debye screening, this diagram contributes at order α_w , and numerical evaluation shows that its contribution to the decay rate of left handed top quarks is comparable to that from the annihilation processes we have considered. However, it only affects left handed top quarks, and even if the rate were infinite it would just share their chemical potential equally with left handed bottom quarks, reducing the friction on the wall by 3/4. (The rate at which thermal top quarks rotate between right and left handed on the wall is smaller than the annihilation rate.) We will neglect this fairly minor effect here.

W boson diagrams

For the W bosons the dominant annihilation processes are t channel conversion to a gluon by a quark and W – gluon fusion to a quark-antiquark pair. Summing over generations, flavors, colors, and particle-antiparticle, we find the matrix element is $\simeq -24g_s^2g_w^2st/(t-m^2)^2$ for each process. (Again we only consider the leading log so $s \simeq -u$.) We will also include order α_w^2 processes, which are double W fusion to fermions, with matrix element $\simeq -18st/(t-m^2)^2$, W scattering from a fermion, with matrix element $120g_w^4s^2/(t-m_W^2)^2$, and absorption re-emission, with matrix element $\simeq -18g_w^4st/(t-m^2)^2$. Scattering from another W boson does not contribute to the decay rates we consider because the sum of particle number, E, and \vec{p} over all particles is zero. These processes do contribute to the damping of higher order perturbations, however, which may help to thermalize infrared W bosons.

We will neglect annihilation to and scattering from the Higgs doublet because the matrix elements are more complicated, because the diagrams introduce infrared problems, and finally and most importantly because there is only one doublet, so its contribution is much smaller than the 12 fermion doublets.

The collision integrals are completely analogous to those discussed above, so we will only present the results. For semi-strong annihilation, we find

$$\frac{6}{\pi^{3}}\alpha_{s}\alpha_{w}T \begin{cases}
(9\zeta_{2}^{2}/16) \ln(9T^{2}/m_{q}^{2}) & \Gamma_{\mu 1} \\
(21\zeta_{2}\zeta_{3}/16) \ln(15T^{2}/m_{q}^{2}) & \Gamma_{\mu 2} \\
(21\zeta_{2}\zeta_{3}/16) \ln(15T^{2}/m_{q}^{2}) & \Gamma_{T 1} \\
(135\zeta_{2}\zeta_{4}/32) \ln(21T^{2}/m_{q}^{2}) & \Gamma_{T 2} \\
(45\zeta_{2}\zeta_{4}/32) \ln(21T^{2}/m_{q}^{2}) & \Gamma_{v}
\end{cases}$$
(89)

For doubly weak annihilation, we find

$$\frac{9}{2\pi^{3}}\alpha_{w}^{2}T \begin{cases}
(9\zeta_{2}^{2}/16)\ln(9T^{2}/\langle m^{2}\rangle) & \Gamma_{\mu 1} \\
(21\zeta_{2}\zeta_{3}/16)\ln(15T^{2}/\langle m^{2}\rangle) & \Gamma_{\mu 2} \\
(21\zeta_{2}\zeta_{3}/16)\ln(15T^{2}/\langle m^{2}\rangle) & \Gamma_{T1} \\
(135\zeta_{2}\zeta_{4}/64)\ln(21T^{2}/\langle m^{2}\rangle) + (49\zeta_{3}^{2}/32)\ln(25T^{2}/\langle m^{2}\rangle) & \Gamma_{T2} \\
(45\zeta_{2}\zeta_{4}/64)\ln(21T^{2}/\langle m^{2}\rangle) & \Gamma_{v}
\end{cases} (90)$$

where $\ln(\langle m^2 \rangle) = 3 \ln(m_q^2)/4 + \ln(m_l^2)/4$.

For collisions from quarks and leptons, we find

$$\frac{15}{2\pi^3}\alpha_w^2 T \begin{cases} 2\zeta_2^2 \ln(25T^2/m_W^2) & \Gamma_{T2} \\ 2\zeta_2^2 \ln(25T^2/m_W^2) & \Gamma_v \end{cases}$$
 (91)

and just as in the case of quarks, scattering diagrams contribute equally to the Γ_{T2} and Γ_v . For absorption and re-emission from fermions, we find

$$\frac{9}{4\pi^3}\alpha_w^2 T \begin{cases} (135\zeta_2\zeta_3/32)\ln(21T^2/\langle m^2\rangle) - (49\zeta_3^2/16)\ln(25T^2/\langle m^2\rangle) & \Gamma_{T2} \\ (45\zeta_2\zeta_3/16)\ln(21T^2/\langle m^2\rangle) - (49\zeta_3^2/48)\ln(25T^2/\langle m^2\rangle) & \Gamma_v \end{cases}$$
(92)

The thermal mass of a left-handed lepton is $m_l^2 = 3g_w^2T^2/32$ plus a small hypercharge correction which we neglect. The results, using $\alpha_w = 1/30$, are $\Gamma_{\mu 1} = 0.00521T$, $\Gamma_{\mu 2} = 0.01012T = \Gamma_{T1}$, $\Gamma_{T2} = 0.03686T$, and $\Gamma_v = 0.01614T$. Annihilations dominate even Γ_v .

13 Appendix B: Critique of the Fluid Approximation

Is the fluid approximation any good?

The discussion can be broken into two parts: does the fluid approximation model properly the energy dependence of δf ; and does it oversimplify the anisotropy of δf ?

We begin with the energy dependence, using the tools developed in Appendix A. Note first that top quarks decay fairly quickly (we have seen that the tails around a source have a length of about 5/T), so a particle excess decays before it is transported off the wall. Hence the friction from one excess particle is roughly its force on the Higgs field at the point where it was created times its lifetime, $\propto \tau/E$. We must determine the behavior of τ .

The annihilation rate of one particle can be computed by putting a bump in the population function f at a specific energy and examining the collision integral. The contribution to δ due to the bump is $-1/f'_0$ times the bump, and $f'_0 = -f_0(1-f_0)$ for a fermion, so the population factor in the collision integral is $f_2(1\pm f_3)(1\pm f_4)/(1-f_1)$ times the bump. The full energy dependence of the collision integral is this expression, the energy conserving delta function, and the $1/E_p$ prefactor. The argument is that $1-f_1$ is quite weakly energy dependent (going from 1/2 at E=0 to 1 at large E where most of the particles are) and for thermal outgoing particles the integral over outgoing states depends on E only through $\ln(2p \cdot k/m_g^2)$, a weak dependence. The dominant dependence is then the 1/E prefactor, which cancels the 1/E strength of the particle's influence on the Higgs field. The argument is strongest for thermal particles, but as they dominate the total friction from top quarks, this should suffice.

Let us check the performance of the fluid approximation for top quarks by neglecting spatial derivatives (ie assuming the particles really do not leave the wall) and comparing the friction from the fluid equations to the friction we would find if we had only included a μ term. Including only a μ term, we find

$$\mu\Gamma_{\mu 1} = v_w c_1 mm'$$
 friction = $c_1 \mu mm'$

The fluid approximation gives

$$\begin{bmatrix} \mu \\ \delta T \end{bmatrix} = \frac{v_w m m'}{\Gamma_{\mu 1} \Gamma_{T2} - \Gamma_{\mu 2} \Gamma_{T1}} \begin{bmatrix} c_1 \Gamma_{T2} - c_2 \Gamma_{T1} \\ c_2 \Gamma_{\mu 1} - c_1 \Gamma_{\mu 2} \end{bmatrix}$$
 friction = $(c_1 \mu + c_2 \delta T) m m'$

Plugging in the values for the Γ 's, the friction is $v_w m^2 m'^2$ times .137 in the first case and .143 in the second case; using the full fluid approximation has only changed our estimate of the friction by 4%. (If the relaxation time approximation were valid the value would have been different by 27%, so the argument must have some validity.) Since we have difficulty trusting our evaluation of the collision integrals to better than 50% (mainly because of the leading log approximation), and since the fluid equations we use should account reasonably well for transport, there seems little reason to improve the fluid approximation for top quarks, except by improving the precision of our evaluation of the collision integrals.

The argument for the fluid approximation also works for thermal W bosons, where $1+f\simeq 1$; but for soft W bosons, the population term in the collision integral is $f_2(1\pm f_3)(1\pm f_4)/(1+f_1)\simeq f_2(1\pm f_3)(1\pm f_4)E/T$, which cancels the 1/E in front of the fluid equations; apparently, the decay rate does not rise as we lower the energy. Evaluating the annihilation and scattering rates of the infrared W bosons is further confused by the appearance of loop diagrams (hard thermal loops) which enter at the same parametric order as tree level effects. Also we should include W boson scattering from other W bosons, which does not contribute to the decay rates we have computed but does contribute to the rate at which infrared particles are thermalized. We will not attempt to treat this problem here, but will only remark that the fluid approximation appears to be a very naive treatment of the W bosons.

Next, we will discuss whether it is acceptable to treat the anisotropy of the distribution keeping only the lowest term, $v \cdot p = pv_iY_{1i}(\hat{p})$, rather than including higher angular moments $p^lY_{lm}(\hat{p})$, where Y_{lm} is a spherical harmonic. The source of δf is isotropic, so \vec{v} only arises out of spatial gradients of δf . The decay of \vec{v} is characterized by the diffusion length $D \simeq 2.7/T$ for quarks (and 5.5/T for W bosons), which is generally smaller than the thickness of the wall. Relative to the other perturbations its amplitude is down by D/L. We expect perturbations at high angular moments to be down by $(D/L)^l$; as long as D is sufficiently less than L, we expect them to be less important than \vec{v} . To confirm this we can extend our treatment beyond the fluid approximation to account for rank two tensor deviations. Setting T=1 for simplicity (we can restore it by dimension counting) and writing

$$f^{-1} = \exp(E - \delta) \pm 1$$

$$\delta = \mu + E\delta T + p_i v_i + E^2 \epsilon + E p_i \epsilon_i + (p_i p_j - \delta_{ij} p^2 / 3) \epsilon_{ij}$$

we find extended fluid equations;

$$c_2\dot{\mu} + c_3\delta\dot{T} + c_4\dot{\epsilon} + \frac{c_3}{3}\partial_i v_i + \frac{c_4}{3}\partial_i \epsilon_i - c_1 m\dot{m} = -\Gamma_{\mu 1}\mu - \Gamma_{T1}\delta T - \Gamma_{\epsilon 1}\epsilon \tag{93}$$

$$c_3\dot{\mu} + c_4\delta\dot{T} + c_5\dot{\epsilon} + \frac{c_4}{3}\partial_i v_i + \frac{c_5}{3}\partial_i \epsilon_i - c_2m\dot{m} = -\Gamma_{\mu 2}\mu - \Gamma_{T2}\delta T - \Gamma_{\epsilon 2}\epsilon \tag{94}$$

$$c_4\dot{\mu} + c_5\delta\dot{T} + c_6\dot{\epsilon} + \frac{\ddot{c_5}}{3}\partial_i v_i + \frac{\ddot{c_6}}{3}\partial_i \epsilon_i - c_3m\dot{m} = -\Gamma_{\mu 3}\mu - \Gamma_{T3}\delta T - \Gamma_{\epsilon 3}\epsilon \tag{95}$$

$$\frac{c_3}{3}\partial_i\mu + \frac{c_4}{3}\partial_i\delta T + \frac{c_5}{3}\partial_i\epsilon + \frac{c_4}{3}\dot{v}_i + \frac{c_5}{3}\dot{\epsilon}_i + \frac{c_5}{15}(\partial_j\epsilon_{ij} + \partial_j\epsilon_{ji} - \frac{2}{3}\partial_i\epsilon_{jj}) \\
= -\Gamma_{v1}v - \Gamma_{\epsilon i1}\epsilon_i \tag{96}$$

$$\frac{c_4}{3}\partial_i\mu + \frac{c_5}{3}\partial_i\delta T + \frac{c_6}{3}\partial_i\epsilon + \frac{c_5}{3}\dot{v}_i + \frac{c_6}{3}\dot{\epsilon}_i + \frac{c_6}{15}(\partial_j\epsilon_{ij} + \partial_j\epsilon_{ji} - \frac{2}{3}\partial_i\epsilon_{jj}) \\
= -\Gamma_{v2}v - \Gamma_{\epsilon i2}\epsilon_i \qquad (97)$$

$$\frac{c_5}{15}(\partial_iv_j + \partial_jv_i - \frac{2\delta_{ij}}{3}\partial_kv_k) + \frac{c_6}{15}(\partial_i\epsilon_j + \partial_j\epsilon_i - \frac{2\delta_{ij}}{3}\partial_k\epsilon_k) + \frac{c_6}{15}(\dot{\epsilon}_{ij} + \dot{\epsilon}_{ji} - \frac{2\delta_{ij}}{3}\dot{\epsilon}_{kk}) = -\Gamma_{\epsilon ij}\epsilon_{ij} \qquad (98)$$

The matrix of Γ 's is block diagonal in angular moments and symmetric. It contains 10 distinct nonzero terms; its evaluation is the main impediment to including higher tensor moments.

Only the isotropic moments μ , δT , and ϵ are directly sourced, since only their time derivatives appear in the equations with the source terms $cm\dot{m}$. The vector moments v_i and ϵ_i are sourced by gradients in the isotropic moments. We expect their amplitudes to be $\sim \mu'/\Gamma \sim \mu D/L$. Similarly, the traceless tensor moment ϵ_{ij} is sourced by gradients in the vector moments, $\partial_i v_j$. Although we have not calculated $\Gamma_{\epsilon ij}$, we anticipate that it will be at least as large as the damping rates for the vector moments, because a particle's contribution to ϵ_{ij} is erased by deflecting the particle by 45°, while it must be deflected by 90° to erase its contribution to v_i . Hence, ϵ_{ij} should be $\sim v_i D/L \sim \mu D^2/L^2$. We conclude that as long as L >> D, the neglect of high order angular moments should be justified. (In the opposite limit, D >> L, we know that, for quarks, the high order moments are very important and lead to a log enhancement of the friction; so L >> D is not only a sufficient condition to neglect high angular moments, but a necessary one.) In our case, $D \simeq 2.7/T$ for top quarks, and we are in good shape. (Even for W bosons, where $D \simeq 5.5/T$, we are in fairly good shape.)

We wish to note that this conclusion relies on the fact that we are interested in the motion of one fluid against another, and not in the dissipation of the motion of a fluid as a whole, or of a fluid of one species. Let us explore this case briefly, to understand the physics of the extended fluid equations. When tracking a one component fluid, or the average over species of a several component fluid, energy and momentum conservation ensure that Γ_{v1} , Γ_{T2} , $\Gamma_{T1} = \Gamma_{\mu 2}$, $\Gamma_{v2} = \Gamma_{\epsilon i1}$, and $\Gamma_{T3} = \Gamma_{\epsilon 2}$ vanish identically, so δT and v_i are not directly dissipated. If in addition there is a nonzero conserved charge density for which μ is the chemical potential, then $\Gamma_{\mu 1}$ and $\Gamma_{\epsilon 1} = \Gamma_{\mu 3}$ also vanish, and μ is not directly dissipated. It is still true that $\epsilon_{ij} \sim v_i D/L$, but now its presence is important, as it is the main source of dissipation in the system. Indeed, if the perturbations are slowly varying, then we can neglect $\dot{\epsilon}_{ij}$ compared to $\partial_i v_j$, et cetera, and solve for the high order perturbations in terms of the lower order ones. We find

$$\epsilon_{ij} = \frac{-c_5}{15\Gamma_{\epsilon ij}} (\partial_i v_j + \partial_j v_i - \frac{2\delta_{ij}}{3} \partial_k v_k)$$

$$\epsilon_i = \frac{-1}{3\Gamma_{\epsilon i2}} (c_5 \dot{v}_i + c_5 \partial_i \delta T + c_4 \partial_i \mu) = \frac{-1}{3\Gamma_{\epsilon i2}} (c_4 - \frac{c_3 c_5}{c_4}) \partial_i \mu$$

$$\epsilon = \frac{-1}{\Gamma_{\epsilon 3}} (\frac{c_5}{3} \partial_i v_i + c_5 \delta \dot{T} + c_4 \dot{\mu})$$

all plus $O(\delta''/\Gamma^2)$. Here we have used Eq. (96) in the equation for ϵ_i . We can also use Eqs. (93) and (94) to simplify the relation for ϵ , but here we should note that the coefficients on $\partial_i v_i$ and $\delta \dot{T}$ only equal in the massless limit. If the mass is zero, then $\epsilon = 0$; otherwise it is $-O(m^2)\partial_i v_i/\Gamma_{\epsilon_3}$.

Substituting these three quantities into the fluid equations for the undamped species, we find

$$c_{2}\dot{\mu} + c_{3}\delta\dot{T} + \frac{c_{3}}{3}\partial_{i}v_{i} = c_{1}m\dot{m} + \frac{c_{4}^{2} - c_{3}c_{5}}{9\Gamma_{\epsilon i2}}\partial^{2}\mu + \frac{O(m^{2})}{\Gamma_{\epsilon 3}}\partial_{i}\dot{v}_{i}$$

$$c_{3}\dot{\mu} + c_{4}\delta\dot{T} + \frac{c_{4}}{3}\partial_{i}v_{i} = c_{2}m\dot{m} + \frac{c_{4}^{2}c_{5} - c_{3}c_{5}^{2}}{9c_{4}\Gamma_{\epsilon i2}}\partial^{2}\mu + \frac{O(m^{2})}{\Gamma_{\epsilon 3}}\partial_{i}\dot{v}_{i}$$

$$\frac{c_{3}}{3}\partial_{i}\mu + \frac{c_{4}}{3}\partial_{i}\delta T + \frac{c_{4}}{3}\dot{v}_{i} = \frac{c_{4}^{2}c_{5} - c_{3}c_{5}^{2}}{9c_{4}\Gamma_{\epsilon i2}}\partial_{i}\dot{\mu} + \frac{O(m^{2})}{\Gamma_{\epsilon 3}}\partial_{i}\partial_{j}v_{j}$$

$$+ \frac{2c_{5}^{2}}{225\Gamma_{\epsilon ij}}\partial_{j}(\partial_{i}v_{j} + \partial_{j}v_{i} - \frac{2\delta_{ij}}{3}\partial_{k}v_{k})$$

$$(99)$$

which are the linearized relativistic Navier-Stokes equations. The perturbations ϵ , ϵ_i , and ϵ_{ij} have caused bulk viscosity, thermal resistivity, and shear viscosity, respectively. The bulk viscosity vanishes in the ultrarelativistic (m << T) limit; the thermal resistivity vanishes in the absence of a nonzero conserved charge density. (In this case heat flow is only resisted by higher derivative terms.)

14 Appendix C: Runaway Wall

According to the tanh *Ansatz*, the wall is capable of becoming ultrarelativistic without contracting to a small plasma frame thickness. We will explore how this arises and why it is unphysical.

First consider the equation of motion in the tanh Ansatz, Eq. (53) and particularly Eq. (55). We see that the derivative term $\Box \phi$ stretches the wall, but that it becomes ineffective at large velocity. One would expect, then, that the wall becomes extremely compressed. But the frictive term Eq. (63) stretches the wall. For a thin wall, where the particles have little time to decay, and at large velocity, where they simply sweep backwards up the wall, we find $\mu \propto \phi^2$ and the ratio of stretching to friction is 11/12. When $\Xi < 5\Delta V_T/6$, then if there is enough friction to stop the wall from accelerating then there is enough to prevent it from contracting to the regime where we can neglect particle decay, so the wall cannot become thinner than about $L \sim 6/T$. When $A_F \neq 0$, the system tends to supercool quite heavily and Ξ tends to be small compared to ΔV_T ; the wall is then susceptible to runaway, according to the tanh Ansatz.

Note that most of the frictive force on the wall comes on the upper part near the symmetric phase. The friction tends to make this part of the wall very thick, as we see explicitly when we solve for the wall shape. What the tanh *Ansatz* does is force the front part of the wall to be as thick as the back, which is unphysical.

Let us attempt an analysis without a wall shape Ansatz. Consider the wall propagating at a steady, very relativistic speed, say $\gamma v_w > 10$. To determine how abrupt the

wall is, we will integrate the equation of motion times ϕ' , starting in the symmetric phase and going up to the point $\phi = \phi_1$; if the wall is in a steady state,

$$\int_{-\infty}^{z:\phi=\phi_1} (V_T'(\phi(z)) + \text{friction})\phi' \, dz = (1 - v_w^2) \int \phi' \phi'' dz = (1 - v_w^2) \frac{(\phi')^2}{2}$$
 (100)

Because $1 - v_w^2$ is very small, the wall is rising very rapidly where $\phi = \phi_1$ unless $V_T(\phi_1) + \int$ friction $\phi' dz$ is almost zero. Let us examine whether this condition is ever satisfied.

First note that the friction is never negative anywhere for a monotonic wall. Now V_T is positive at small ϕ , as otherwise the phase transition would have already proceeded by spinodal decomposition. So there will be a section at the front of the wall where ϕ' is large, ie a section which is very abrupt. To determine where this section ends, we need to find \int friction $\phi' dz$ on this section of wall.

This is easy in the fluid approximation. As the wall is thin, we can neglect decays, and the fluid equations can be integrated. The friction is, in the notation of section 8, $f_i(A^{-1})_{ij}F_j\phi_1^4/8$. Adding this to the effective potential, we get a curve whose second minimum lies above 0 for the effective potential parameters in Table 1 with $A_F = 0.1$ or 0.2, but whose second minimum is below 0 for $A_F = 0.3$. In the former case, the whole wall is abrupt and feels a net backwards force; the wall will then slow down until it is not abrupt and no runaway occurs. In the latter case, a section of the wall feels a net forward pressure, and accelerates without limit. According to the fluid approximation, the wall will run away in these cases.

When the wall becomes this thin, the fluid approximation is definitely inaccurate—as we have argued, it only makes sense when the wall is thicker than the diffusion length. The free particle approximation should be appropriate, however, and for an ultrarelativistic wall we can make an accurate expansion in large γ .

The total pressure on this section of wall from one species is, in the free particle, 1 loop approximation ([5, 19])

$$\int_{m}^{\infty} \frac{dp_{z}}{2\pi} (p_{z} - \sqrt{p_{z}^{2} - m^{2}}) \int \frac{d^{2}p_{\perp}}{(2\pi)^{2}} \frac{p_{z}}{\sqrt{p_{z}^{2} + p_{\perp}^{2}}} \frac{1}{\exp(\beta\gamma(p - vp_{z})) \pm 1} + \int_{0}^{m} \frac{dp_{z}}{2\pi} 2p_{z} \int \frac{d^{2}p_{\perp}}{(2\pi)^{2}} \frac{p_{z}}{\sqrt{p_{z}^{2} + p_{\perp}^{2}}} \frac{1}{\exp(\beta\gamma(p - vp_{z})) \pm 1} + (101)$$

$$\int_{0}^{\infty} \frac{dp_{z}}{2\pi} (-p_{z} + \sqrt{p_{z}^{2} + m^{2}}) \int \frac{d^{2}p_{\perp}}{(2\pi)^{2}} \frac{p_{z}}{\sqrt{p_{z}^{2} + p_{\perp}^{2} + m^{2}}} \frac{1}{\exp(\beta\gamma(\sqrt{p^{2} + m^{2}} + vp_{z})) \pm 1}$$

where m is the particle mass when $\phi = \phi_1$.

Taking $\gamma >> T/m$ so that $\exp(-\gamma m/T) << m^2/T^2$, we find the friction is

$$\frac{m^2 T^2}{48} + \frac{m^3 T \ln 2}{12\pi^2 \gamma} - \frac{m^2 T^2}{192\gamma^2} + O(m^4 \ln(\gamma T/m)/\gamma^2)$$
 (102)

from a fermion degree of freedom and

$$\frac{m^2 T^2}{24} + \frac{m^3 T}{4\pi^2 \gamma} \left(-\frac{5}{18} - .1347 + \frac{\ln(2\gamma T/m)}{3} \right) - \frac{m^2 T^2}{96\gamma^2} + O(m^4 \ln(\gamma T/m)/\gamma^2) \quad (103)$$

from a boson⁴. Subtracting from these the corresponding 1 loop contributions to the effective potential,

$$\frac{m^2 T^2}{48} - \frac{m^4}{32\pi^2} \left(\ln(\pi T/m) - \gamma_E + .75 \right) , \qquad \frac{m^2 T^2}{24} - \frac{m^3 T}{12\pi}$$
 (104)

gives the friction from particles on the abrupt part of the wall, at 1 loop. This friction is much larger than the prediction of the fluid approximation. Adding this expression to V_T produces a function which is positive for all $\phi_1 > 0$, for all values of the effective potential parameters we have considered; in fact it comes quite far from having a second zero. This means that there is no value of ϕ where the abrupt part of the wall can end; it always has a net backwards force on it, even when $\phi_1 = \phi_0$. It is simply impossible to have an ultrarelativistic, steady state solution to the wall shape. As the wall becomes very fast, the front of the wall always compresses and sustains enough friction to prevent further acceleration. We cannot determine the velocity of the wall, but we can say that it must be slow enough that the free particle approximation is inaccurate, which ensures that γv_w cannot be much greater than 1. Note that it was not necessary for the condensate responsible for A_F to exert any friction for this to be true.

References

- [1] G. t'Hooft, Phys. Rev. **D14**, 3432 (1976)
- [2] V. Kuzmin, V. Rubakov, and M. Shaposhnikov, Phys. Lett. 155B, 36 (1985)
- [3] P. Arnold and L. McLerran, Phys. Rev. **D** 36, 581 (1987)
- [4] D. Krizhnits and A. Linde, Ann. Phys. 101, 195 (1976)
- [5] M. Dine, R.G. Leigh, P. Huet, A. Linde, and D. Linde, Phys. Rev D 46, 550 (1992)
- [6] P. Arnold and O. Espinoza, Phys. Rev. **D** 47, 3546 (1993)
- [7] Z. Fodor and A. Hebecker, Nucl. Phys. **B432**, 127 (1994)
- [8] M. Shaposhnikov, Phys. Lett. **B 316**, 112 (1993)
- [9] K. Farakos, K. Kajantie, K. Rummukainen, and M. Shaposhnikov, Nuclear Phys. B 425, 67 (1994); Phys. Lett. B 336, 494 (1994); CERN preprint CERN-TH-7220-94, hep-lat/9412091
- [10] B. Bergerhoff and C. Wetterich, preprint HD-THEP-94-31, hep-ph/9409295
- [11] F. Sisikor et. al., hep-lat/9411052; Z. Fodor, hep-lat/9503014

^{4.1347097} is the numerical value of $\int_1^\infty (x^2 - x\sqrt{x^2 - 1} - 1/2) \ln x \, dx$, which we reduced to $-\sum_{n=2} \Gamma(n-1/2)/(\Gamma(-1/2)\Gamma(n+1)(2n-3)^2)$ but were unable to reduce further.

- [12] A. Cohen, D. Kaplan, and A. Nelson, Phys. Lett. **245B**, 561 (1990)
- [13] A. Nelson, D. Kaplan, and A. Cohen, Nucl. Phys. **B373**, 453 (1992)
- [14] M. Joyce, T. Prokopec, and N. Turok, Princeton preprint PUPT-94-1495, hep-ph/9410281
- [15] N. Turok and J. Zadrozny, Phys. Rev. Lett. 65, 2331 (1990), Nuc. Phys. B 358, 471 (1991)
- [16] M. Joyce, T. Prokopec, and N. Turok, Princeton preprint PUPT-94-1496, hep-ph/9410282
- [17] A. Cohen, D. Kaplan, and A. Nelson, Phys. Lett. **B263**, 86 (1991)
- [18] N. Turok, Phys. Rev. Lett. 68, 1803 (1992).
- [19] B. H. Liu, L. McLerran, and N. Turok, Phys. Rev. **D** 46, 2668 (1992)
- [20]
- [21] P. Arnold, Phys. Rev. **D** 48, 1539 (1993)
- [22] G. Moore and T. Prokopec, Phys. Rev. Lett., in print;
- [23] S. Coleman, Phys. Rev. **D15**, 2929 (1977); S. Coleman and C. Callan, Phys. Rev. **D16**, 1762 (1977)
- [24] J. Ignatius, K. Kajantie, H. Kurki-Suonio and M. Laine, Phys. Rev. D 49, 3854 (1994); K. Enqvist, J. Ignatius, K. Kajantie and K. Rummukainen, Phys. Rev. D 45, 3415 (1992)
- [25] M. Carrington and J. Kapusta, Phys. Rev. **D47**, 5304 (1993)
- [26] A. F. Heckler, Phys. Rev. **D** 51, 405 (1995)
- [27] A. D. Linde, Phys. Lett. **96B**, 289 (1980)
- [28] M. Carrington, Phys. Rev. **D45**, 2933 (1992) e-Print Archive: hep-ph/9503296
- [29] A.D. Linde, Phys. Lett. **70B** (1977) 306; **100B** (1981) 37; Nucl. Phys. **B216** (1983) 421.
- [30] G. Anderson and L. Hall, Phys. Rev. **D** 45, 2685 (1992)
- [31] A. Guth and S. Tye, Phys. Rev. Lett. 44, 613 (1980); A. Guth and E. Weinberg, Phys. Rev. D 23, 816 (1981)
- [32] H. Weldon, Phys. Rev. **D28**, 2007 (1983)
- [33] Braaten and Pisarski, Phys. Rev. **D42**, 2156 (1990)

- [34] H. Weldon, Phys. Rev. **D26**, 2789 (1982)
- [35] E.V. Shuryak, JETP 47 (1978) 212; O.K. Kalashnikov and V.V. Klimov, Sov.
 J. Nucl. Phys. 31 (1980) 699; H.A. Weldon, Phys. Rev. D26 (1982) 1384, 2789
- [36] these values differ slightly from those in [22] because there we used a slightly different approximation in Eq. (80), evaluated the scattering integrals numerically rather than analytically, and made a slight error in the absorption-reemission diagram. The difference is insignificant.

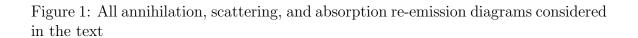


Figure 2: Plot of the solutions of Eq. (53) for the case $\lambda_T = 0.03$, $A_F = 0$. The solid line is the velocity constraint and the dotted line is the thickness constraint.

Figure 3: Wall shape; at left, for $\lambda_T=0.04$, $A_F=0.1$, and at right, for $\lambda_T=0.03$, $A_F=0$. The solid line is the numerical value, the dotted line is the tanh Ansatz shape. The scale is the same for both; the full width of the pictures are 96/T and 64/T.